A potential-free field inverse time-fractional Schrödinger problem: optimal error bound analysis and regularization method*

Fan Yang†, Jun-Liang Fu, Xiao-Xiao Li
School of Science, Lanzhou University of Technology,
Lanzhou, Gansu, 730050, People's Republic of China

Abstract: In this paper, an inverse time-fractional Schrödinger problem of potential-free field is studied. This problem is ill-posed, i.e, the solution (if it exists) does not depend continuously on the data. Based on an a priori bound condition, the optimal error bound analysis is given. Moreover, a modified kernel method is introduced. The convergence error estimate obtained by this method under the priori regularization parameter selection rule is optimal, and the convergence error estimate obtained under the posteriori regularization parameter selection rule is order-optimal. Finally, some numerical examples are given to illustrate the effectiveness and stability of this method.
keywords: Time-fractional Schrödinger equation; Optimal error bound; A modified kernel method; Ill-posed problem; Inverse Problem
MSC: 65M32; 35R11

1 Introduction

Schrödinger equation is the basic equation of quantum mechanics, which reveals the basic law of material movement in the micro physical world. It has important applications in physical phenomena such as optical pulse propagation, superconductivity, wave in water and plasma, and self-focusing in laser pulse. Recently, there are many methods to study the positive problem of Schrödinger equation [1–15]. For the inverse Schrödinger problem has been studied by many scholars. Eskin [16] proves the uniqueness of time-varying EMF determination for Schrödinger equation with obstacle region from Dirichlet-to-Neumann mapping. Rakesh and Symes [17] prove that the Dirichlet-to-Neumann map uniquely determines the time-independent potential in the wave equation. Cipolatti and Lopez [18] consider the inverse problem of restoring time-independent damping coefficients in the wave equation from Dirichlet to Neumann mapping. In [19], Cheng and Yamamoto prove the stability estimate and give the convergence rate of Tikhonov regularization solution. For two-dimensional inverse boundary value problems, see [20–24].

*The project is supported by the National Natural Science Foundation of China (No. 11961044), the Distinguished Young Scholars Fund of Lan Zhou University of Technology.

†E-mail addresses: yfggd114@163.com.

Fractional equation has many natural advantages, such as simple modeling, clear physical meaning and accurate description, and is widely used in various research fields. For the fractional Schr$\ddot{o}$dinger equation, Laskin [25] derives a space-fractional Schr$\ddot{o}$dinger equation with the Laplace operator instead of the quantum Riesz derivative by using the Feynman path integrals over the Levy trajectories. In [26], Naber proposed and discussed a different generalization method, which converted the first order time-derivative into Caputo fractional derivative, and studied two different generalization methods. And for the numerical solution of the time fractional Schr$\ddot{o}$dinger equation, see [27, 28]. However, few researchers have studied the inverse problem of time-fractional Schr$\ddot{o}$dinger equation.

There are many regularization methods for the study of inverse problems, such as Tikhonov regularization method [29], quasi-boundary value method [30], quasi-reversibility regularization method [31, 32], a mollification regularization method [33], Fourier regularization method [34–36], Landweber iterative regularization method [37, 38] and so on. In this paper, we consider the following the potential-free field inverse time-fractional Schr$\ddot{o}$dinger problem with boundary condition

$$\begin{cases} i\, {}_0^C D_t^{\alpha} u(x,t) + u_{xx}(x,t) = 0, & x > 0,\ t > 0, \\ u(x,0) = 0, & x \geq 0, \\ u(1,t) = f(t), & t \geq 0, \\ u(x,t) \mid_{x\to\infty} bounded, & t > 0, \end{cases} \tag{1.1}$$

where $i = \sqrt{-1}$ is the imaginary unit and ${}_0^C D_t^{\alpha}$ is the Caputo time-fractional derivative of order α defined as

$${}_0^C D_t^{\alpha} u(x,t) = \frac{1}{\Gamma(1-\alpha)} \int_0^t (t-\tau)^{-\alpha} u_{\tau}(x,\tau) d\tau, \quad 0 < \alpha < 1,$$

in which $\Gamma(\cdot)$ is the Gamma function.

In problem (1.1), we wish to reconstruct the wave function $u(x,t)$ for $0 \leq x < 1$ according to the measured data function $f^{\delta}(t)$.

We will prove that the inverse time-fractional Schr$\ddot{o}$dinger problem is ill-posed and introduce a modified kernel method [39] to compute $u(x,t)(0 \leq x < 1)$. We find that under the rules of priori and posteriori regularization parameter selection, the priori estimates obtained by the modified kernel method are optimal, and the posteriori estimates are order-optimal. Finally, some examples are given to illustrate the effectiveness of this method.

The manuscript is organized as follows. In the second section, we use Fourier transform to obtain the exact solution and prove the ill-posedness of the problem (1.1). In the third section, we draw into preliminary result and optimal error bound for problem (1.1). Above all, we introduce a modified kernel method, and give the convergence estimates between exact solutions and regularization solutions under priori and posteriori regularization parameter selection rules in the fourth section. In the fifth section, the analysis of the optimal approximation of this regularization methods are solved. Some numerical examples are given in the sixth part. The seventh section makes a brief conclusion.

2 Ill-posed analysis

In this section, we mainly apply the Fourier transform techniques to study the ill-posedness of the problem (1.1). In order to use the Fourier transform techniques, we extend the definition domain of function $u(x,t)$, $f(t)$ and $f^{\delta}(t)$ to the whole real field $\mathbb{R}$, and set the function to be zero under $t < 0$.

We assume that the exact data function $f(t) \in L^2(\mathbb{R})$ and the measurement data function $f^\delta(t) \in L^2(\mathbb{R})$ satisfy

$$\|f(\cdot) - f^\delta(\cdot)\| \le \delta, \tag{2.1}$$

where $\|\cdot\|$ denotes the $L^2(\mathbb{R})$-norm and $\delta > 0$ is the noise level.

Let

$$\hat{f}(\xi) = \frac{1}{\sqrt{2\pi}} \int_{-\infty}^{+\infty} f(t) e^{-i\xi t} dt, \quad \xi \in \mathbb{R}$$

be the Fourier transform of a function $f(t)$. Taking the Fourier transform to Equations (1.1) with respect to t, by a simple calculation, we obtain the solution of Equations (1.1) in the frequency domain

$$\hat{u}(x,\xi) = e^{(1-x)\sqrt{-i(i\xi)^\alpha}} \hat{f}(\xi), \quad 0 \le x < 1, \tag{2.2}$$

where

$$(i\xi)^\alpha = |\xi|^\alpha (\cos(\frac{\alpha\pi}{2}) + i sign(\xi) \sin(\frac{\alpha\pi}{2})).$$

Denote $\theta(\xi)$ as follows

$$\theta(\xi) := \sqrt{-i(i\xi)^\alpha} = \Phi(\xi) + i\Psi(\xi), \tag{2.3}$$

where

$$\Phi(\xi) := \sqrt{\frac{|\xi|^\alpha (1 + sign(\xi) \sin(\frac{\alpha\pi}{2}))}{2}},$$

$$\Psi(\xi) := -\sqrt{\frac{|\xi|^\alpha (1 - sign(\xi) \sin(\frac{\alpha\pi}{2}))}{2}}.$$

In accordance with (2.3), the expression (2.2) is redefined as follows

$$\hat{u}(x,\xi) = e^{(1-x)\theta(\xi)} \hat{f}(\xi), \quad 0 \le x < 1. \tag{2.4}$$

Using inverse Fourier transform, we obtain the exact solution

$$u(x,t) = \frac{1}{\sqrt{2\pi}} \int_{-\infty}^{+\infty} e^{(1-x)\theta(\xi)} \hat{f}(\xi) e^{i\xi t} d\xi, \quad 0 \le x < 1. \tag{2.5}$$

From above formula (2.5), since $|e^{(1-x)\theta(\xi)}|$ is unbounded with respect to variables ξ, the small errors in the high frequency components will be amplified. Therefore, this inverse problem is a serious ill-posed problem, which requires a feasible regularization method.

Suppose $u(0,t)$ satisfies the a-priori bound condition

$$\|u(0,t)\|_{M^p(\mathbb{R})} \le E, \quad p \ge 0, \tag{2.6}$$

where E is a positive constant and $\|\cdot\|_{M^p(\mathbb{R})}$ is defined with the norm

$$\|u(0,t)\|_{M^p(\mathbb{R})} := \Big(\int_{-\infty}^{+\infty} e^{p\Phi(\xi)} |\hat{u}(0,\xi)|^2 d\xi \Big)^{\frac{1}{2}}. \tag{2.7}$$

Remark 2.1. *When $p = 0$, we can know that $M^p(\mathbb{R}) = M^0(\mathbb{R}) = L^2(\mathbb{R})$ and formula (2.6) is bounded in the $L^2(\mathbb{R})$-norm.*

3 Preliminary result and optimal error bound

3.1 Preliminary result

We consider arbitrary ill-posed inverse problems [40–44]:

$$Ax = y, \tag{3.1}$$

where $A \in \mathcal{L}(X, Y)$ is a linear bounded between infinite dimensional Hilbert spaces X and Y with non-closed range $R(A)$ of A. Assume that $y^\delta \in Y$ are available noisy data with $\|y - y^\delta\| \le \delta$. Any operator $R : Y \to X$ can be considered as a special method for approximately solving (3.1), and the approximate solution of (3.1) is given by Ry^δ.

Let $M \subset X$ be a bounded set. Let us introduce the worst case error $\Delta(\delta, R)$ for identifying x from y^δ as [40–43]

$$\Delta(\delta, R) := \sup\{\|Ry^\delta - x\| | x \in M, y^\delta \in Y, \|Kx - y^\delta\| \le \delta\}. \tag{3.2}$$

The best possible error bound (or optimal error bound) is defined as the infimum over all mappings $R : Y \to X$:

$$\omega(\delta) := \inf_R \Delta(\delta, R). \tag{3.3}$$

Now let us review some optimality results if the set $M = M_{\varphi,E}$ is given by

$$M_{\varphi,E} = \{x \in X | x = [\varphi(A^*A)]^{\frac{1}{2}} v, \|v\| \le E\}, \tag{3.4}$$

where the operator function $\varphi(A^*A)$ is well defined via spectral representation [42], [45], [46]

$$\varphi(A^*A) = \int_0^a \varphi(\lambda) dE_\lambda, \tag{3.5}$$

where $A^*A = \int_0^a \lambda dE_\lambda$ is the spectral decomposition of A^*A, E_λ denotes the spectral family of the operator A^*A, and a is a constant such that $\|A^*A\| \le a$ with $a = \infty$ if A^*A is unbounded. In the case when $A : L^2(\mathbb{R}) \to L^2(\mathbb{R})$ is a multiplication operator, $Ax(s) = \gamma(s)x(s)$, the operator function $\varphi(A^*A)$ has the form

$$\varphi(A^*A)x(s) = \varphi(|\gamma(s)|^2)x(s). \tag{3.6}$$

Then a method R_0 is called [43]

(i) optimal on the set $M_{p,E}$ if $\Delta(\delta, R_0) = \omega(\delta, E)$ holds;

(ii) order optimal on the set $M_{p,E}$ if $\Delta(\delta, R_0) \le C\omega(\delta, E)$ with $C \ge 1$ holds.

In order to derive an explicit (best possible) optimal error bound for the worst case error $\Delta(\delta, R)$ defined in (3.2), we assume that the function φ in (3.6) satisfies the following assumption:

Assumption 3.1. *([42, 43, 46])The function $\varphi(\lambda) : (0, a] \to (0, \infty)$ in (3.6), where a is a constant such that $\|A^*A\| \le a$, is continuous and has the following properties:*

(i) $\lim_{\lambda \to 0} \varphi(\lambda) = 0$;

(ii) φ is strictly monotonically increasing on $(0, a]$;

(iii) $\rho(\lambda) = \lambda\varphi^{-1}(\lambda) : (0, \varphi(a)] \to (0, a\varphi(a)]$ *is convex.*

Under **Assumption** 3.1, the next theorem gives us a general formula for the optimal error bound.

Theorem 3.1. *([42, 43, 46])Let $M_{\varphi,E}$ be given by (3.4), let **Assumption** 3.1 be satisfied, and let $\frac{\delta^2}{E^2} \in \sigma(A^*A\varphi(A^*A))$, where $\sigma(A^*A)$ denotes the spectrum of operator A^*A, then*

$$\omega(\delta, E) = E\sqrt{\rho^{-1}(\frac{\delta^2}{E^2})}. \tag{3.7}$$

3.2 Optimal error bound

In this section we consider problem (1.1) and deal with the question concerning the best possible worst case error (3.3) for identifying $u(x,t)(0 \le x < 1)$ from noisy data $f^\delta(t) \in L^2(\mathbb{R})$ provided (2.1) and $u(x,t) \in M_{p,E}$ hold, where $M_{p,E}$ is given by

$$u(x,t) \in M_{p,E} = \{u(x,t) \in L^2(\mathbb{R}) | \|u(0,t)\|_{M^p(\mathbb{R})} \le E, p \ge 0\}, \tag{3.8}$$

where $\|\cdot\|_{M^p(\mathbb{R})}$ is defined with the norm

$$\|u(0,t)\|_{M^p(\mathbb{R})} := \Big(\int_{-\infty}^{+\infty} e^{p\Phi(\xi)}|\hat{u}(0,\xi)|^2 d\xi\Big)^{\frac{1}{2}}. \tag{3.9}$$

Let us formulate problem (1.1) as an operator equation

$$Au(x,t) = f(t), \quad 0 \le x < 1, \tag{3.10}$$

with linear operator $A \in \mathcal{L}(L^2(\mathbb{R}), L^2(\mathbb{R}))$. Obviously, this equation is equivalent to the operator equation in the frequency space

$$\hat{A}\hat{u}(x,\xi) = \hat{f}(\xi), \quad \hat{A} = \mathcal{F}A\mathcal{F}^{-1}, \tag{3.11}$$

where $\mathcal{F} : L^2(\mathbb{R}) \to L^2(\mathbb{R})$ is the (unitary) Fourier transformation operator that maps any function $v(t) \in L^2(\mathbb{R})$ into its Fourier transform $\hat{v}(\xi)$. From (2.2), we obtain

$$e^{-(1-x)\theta(\xi)}\hat{u}(x,\xi) = \hat{f}(\xi). \tag{3.12}$$

So

$$\hat{A} = e^{-(1-x)\theta(\xi)}, \tag{3.13}$$

which shows that $\hat{A} : L^2(\mathbb{R}) \to L^2(\mathbb{R})$ in (3.11) is a linear and bounded multiplication operator, where the inverse $\hat{A}^{-1}$ is unbounded. Since $\hat{A}^* = e^{-(1-x)\overline{\theta(\xi)}}$, we have

$$\hat{A}\hat{A}^* = \hat{A}^*\hat{A} = e^{-2(1-x)\Phi(\xi)}. \tag{3.14}$$

The smoothness condition (3.8) can also be transformed into an equivalent condition in the frequency domain. From (3.9) we have that condition (3.8) is equivalent to the condition

$$\hat{u}(x,\xi) \in \hat{M}_{p,E} = \{\hat{u}(x,\xi) \in L^2(\mathbb{R}) | \|\hat{u}(0,\xi)\|_{M^p(\mathbb{R})} \le E, p \ge 0\}, \tag{3.15}$$

where

$$\|\hat{u}(0,\xi)\|_{M^p(\mathbb{R})} := \Big(\int_{-\infty}^{+\infty} e^{p\Phi(\xi)}|\hat{u}(0,\xi)|^2 d\xi\Big)^{\frac{1}{2}}. \tag{3.16}$$

This condition can be reformulated into an equivalent condition with a set of the structure (3.4).

Proposition 3.1. *Consider the operator equation* (3.11)*. Then the set* $\hat{M}_{p,E}$ *given in* (3.15) *is equivalent to the general source set*

$$\hat{M}_{\varphi,E} = \{\hat{u}(x,\xi) \in L^2(\mathbb{R})|, \|[\varphi(A^*A)]^{-\frac{1}{2}}\hat{u}(x,\xi)\| \le E\}, \tag{3.17}$$

where $\varphi = \varphi(\lambda)$ *is given (in parameter representation) by*

$$\begin{cases} \lambda(r) = e^{-2(1-x)r}, \\ \varphi(r) = e^{-(p+2x)r}, \end{cases} \qquad 0 \le r < \infty. \tag{3.18}$$

Proof. From (2.4), we have $\hat{u}(x,\xi) = e^{-x\theta(\xi)}\hat{u}(0,\xi)$. Comparing (3.15) with (3.17), we obtain

$$\varphi(\hat{A}^*\hat{A})) = e^{-(p+2x)\Phi(\xi)}. \tag{3.19}$$

From this representation and (3.14), we obtain that φ is given (in parameter representation) by $\lambda(\xi) = e^{-2(1-x)\Phi(\xi)}, \varphi(\xi) = e^{-(p+2x)\Phi(\xi)}, \xi \in \mathbb{R}$. We substitute $\Phi(\xi) = r$ and obtain (3.18). ■

We will discuss properties of the function $\varphi = \varphi(\lambda)(\lambda \in (0,\infty))$ which is given (in parameter representation) by (3.18) in the following.

Proposition 3.2. *The function* $\varphi(\lambda)$ *defined by* (3.18) *is continuous and has the following properties:*
Case 1: *when* $p = 0$ *and* $0 < x < 1$*, there holds*

(i) $\lim_{\lambda\to 0}\varphi(\lambda) = 0$*;*

(ii) φ *is strictly monotonically increasing;*

(iii) $\rho(\lambda) = \lambda\varphi^{-1}(\lambda)$ *is strictly monotonically increasing and possesses the following parameter representation:*

$$\begin{cases} \lambda(r) = e^{-2xr}, \\ \rho(r) = e^{-2r}, \end{cases} \qquad 0 \le r < \infty. \tag{3.20}$$

(iv) $\rho^{-1}(\lambda)$ *is strictly monotonically increasing and possesses the following parameter representation:*

$$\begin{cases} \lambda(r) = e^{-2r}, \\ \rho^{-1}(r) = e^{-2xr}, \end{cases} \qquad 0 \le r < \infty. \tag{3.21}$$

(v) For the inverse function $\rho^{-1}(\lambda)$*, there holds*

$$\rho^{-1}(\lambda) = \lambda^x, \quad for\ \lambda \to 0. \tag{3.22}$$

Case 2: *when* $p > 0$ *and* $x = 0$*, there holds*

(i) $\lim_{\lambda\to 0}\varphi(\lambda) = 0$*;*

(ii) φ *is strictly monotonically increasing;*

(iii) $\rho(\lambda) = \lambda\varphi^{-1}(\lambda)$ *is strictly monotonically increasing and possesses the following parameter representation:*

$$\begin{cases} \lambda(r) = e^{-pr}, \\ \rho(r) = e^{-(p+2)r}, \end{cases} \qquad 0 \le r < \infty. \tag{3.23}$$

(iv) $\rho^{-1}(\lambda)$ is strictly monotonically increasing and possesses the following parameter representation:

$$\begin{cases} \lambda(r) = e^{-(p+2)r}, \\ \rho^{-1}(r) = e^{-pr}, \end{cases} \qquad 0 \le r < \infty. \tag{3.24}$$

(v) For the inverse function $\rho^{-1}(\lambda)$, there holds

$$\rho^{-1}(\lambda) = \lambda^{\frac{p}{p+2}}, \quad for\ \lambda \to 0. \tag{3.25}$$

Proof. The proof of (i), (ii), (iii) and (iv) are obvious in **Case 1** and **Case 2**. We only give the proof of (v).
For **case 1**, let $F_1(\lambda) = \rho^{-1}(\lambda)\lambda^{-x}$, we can obtain

$$\begin{aligned} \lim_{\lambda \to 0} F_1(\lambda) &= \lim_{r \to \infty} e^{-2xr}(e^{-2r})^{-x} \\ &= \lim_{r \to \infty} e^{-2xr+2xr} \\ &= 1. \end{aligned}$$

For **case 2**, let $F_2(\lambda) = \rho^{-1}(\lambda)\lambda^{-\frac{p}{p+2}}$, we have

$$\begin{aligned} \lim_{\lambda \to 0} F_2(\lambda) &= \lim_{r \to \infty} e^{-pr}(e^{-(p+2)r})^{-\frac{p}{p+2}} \\ &= \lim_{r \to \infty} e^{-pr+pr} \\ &= 1. \end{aligned}$$

The proof of (3.22) and (3.25) are completed. ■

Proposition 3.3. *The function $\rho(\lambda)$ defined by (3.20) and (3.23) are strictly convex.*

Proof. The proof is similar to [42, 43, 46, 47], and we omit it. ■

Now we will formulate our main result of this section concerning the best possible worst case error $\omega(\delta, E)$ defined in (3.2) for identifying the solution $u(x,t)(0 \le x < 1)$ of problem (1.1) from noisy data $f^\delta(t) \in L^2(\mathbb{R})$ under condition (2.1) and $u(x,t) \in M_{p,E}$, where the set $M_{p,E}$ is given by (3.8). Since the Fourier operator $\mathcal{F}$ is unitary (i.e. $\mathcal{F}^{-1} = \mathcal{F}^*$), we introduce the optimal error bound by

$$\omega(\delta, E) = \hat{\omega}(\delta, E) := \inf \sup\{\|\hat{R}\hat{f}^\delta - \hat{u}(x,\cdot)\| | \hat{u}(x,\cdot) \in \hat{M}_{p,E}, \hat{f}^\delta \in L^2(\mathbb{R}), \|\hat{f} - \hat{f}^\delta\| \le \delta\}, \tag{3.26}$$

where $\hat{R}$ is an arbitrary method for approximately solving (3.11), and " inf " means the minimum over all methods $\hat{R} : L^2(\mathbb{R}) \to L^2(\mathbb{R})$.

Theorem 3.2. *Suppose conditions (2.1) and (3.17) hold. Then the optimal error bound for solving problem (1.1) is:*
(i) *in case $p = 0$ and $0 < x < 1$, there holds*

$$\omega(\delta, E) = \delta^x E^{1-x}. \tag{3.27}$$

(ii) *in case $p > 0$ and $x = 0$, there holds*

$$\omega(\delta, E) = \delta^{\frac{p}{p+2}} E^{\frac{2}{p+2}}. \tag{3.28}$$

Proof. Combining (3.7) with (3.22) and (3.25), for **(i)**, we get

$$\begin{aligned}\omega(\delta,E) &= E\sqrt{\rho^{-1}(\frac{\delta^2}{E^2})}\\ &= E\sqrt{(\frac{\delta^2}{E^2})^x}\\ &= \delta^x E^{1-x}.\end{aligned}$$

For **(ii)**, we have

$$\begin{aligned}\omega(\delta,E) &= E\sqrt{\rho^{-1}(\frac{\delta^2}{E^2})}\\ &= E\sqrt{(\frac{\delta^2}{E^2})^{\frac{p}{p+2}}}\\ &= \delta^{\frac{p}{p+2}} E^{\frac{2}{p+2}}.\end{aligned}$$

The proof is completed. ■

4 A modified kernel method and convergence rates

In this section, we propose a modified kernel method to solve the ill-posed problem (1.1) and give the convergence estimates. The regularization solution is given by

$$\hat{u}_\mu^\delta(x,\xi) = k_\mu(x,\xi)\hat{f}^\delta(\xi), \quad 0 \le x < 1, \tag{4.1}$$

where

$$k_\mu(x,\xi) = \begin{cases} e^{(1-x)(\Phi(\xi)+i\Psi(\xi))}, & e^{(1-x)\Phi(\xi)} \le \mu(x),\\ \mu(x)e^{i(1-x)\Psi(\xi)}, & e^{(1-x)\Phi(\xi)} > \mu(x),\end{cases} \tag{4.2}$$

where $\mu(x) > 1$ is the regularization parameter.

According to the inverse Fourier transform, we obtain regularization solution

$$u_\mu^\delta(x,t) = \frac{1}{\sqrt{2\pi}}\int_{-\infty}^{+\infty} k_\mu(x,\xi)\hat{f}^\delta(\xi)e^{i\xi t}d\xi, \quad 0 \le x < 1. \tag{4.3}$$

Next, we give two error estimates under an a priori regularization parameter choice rule and an a posteriori parameter choice rule.

4.1 The error estimate with a priori parameter choice

Theorem 4.1. *Suppose that $u_\mu^\delta(x,t)$ given by (4.3) is the regularization solution of the exact solution (2.5). Let $p = 0$ and let the assumption (2.1) and (2.6) be satisfied. If we choose*

$$\mu(x) = x\Big(\frac{E}{\delta}\Big)^{1-x}, \tag{4.4}$$

then for every $x \in (0,1)$, we obtain the following error estimate

$$\|u_\mu^\delta(x,t) - u(x,t)\| \le \delta^x E^{1-x}. \tag{4.5}$$

Proof. Due to the Parseval's identity and the triangle inequality, we have

$$\begin{aligned}\|u_\mu^\delta(x,t)-u(x,t)\| &= \|\hat{u}_\mu^\delta(x,\xi)-\hat{u}(x,\xi)\| \\ &\le \|\hat{u}_\mu^\delta(x,\xi)-\hat{u}_\mu(x,\xi)\|+\|\hat{u}_\mu(x,\xi)-\hat{u}(x,\xi)\| \\ &= \|k_\mu(x,\xi)\hat{f}^\delta-k_\mu(x,\xi)\hat{f}\|+\|k_\mu(x,\xi)\hat{f}-\hat{u}(x,\xi)\| \\ &= I_1+I_2.\end{aligned} \tag{4.6}$$

For I_1, we can deduce that

$$I_1=\|k_\mu(x,\xi)\hat{f}^\delta-k_\mu(x,\xi)\hat{f}\|=\|k_\mu(x,\xi)(\hat{f}^\delta-\hat{f})\|\le\sup_{\xi\in\mathbb{R}}|k_\mu(x,\xi)|\delta\le\delta\mu(x). \tag{4.7}$$

From (2.4), we obtain $\hat{u}(0,\xi)=e^{\theta(\xi)}\hat{f}(\xi)$ and $\hat{u}(x,\xi)=e^{-x\theta(\xi)}\hat{u}(0,\xi)$. Hence, we have

$$\begin{aligned}I_2&=\|(k_\mu(x,\xi)e^{-\theta(\xi)}-e^{-x\theta(\xi)})\hat{u}(0,\xi)\| \\ &=\Big\|\frac{k_\mu(x,\xi)-e^{(1-x)(\Phi(\xi)-i\Psi(\xi))}}{e^{\Phi(\xi)-i\Psi(\xi)}}\hat{u}(0,\xi)\Big\| \\ &\le\sup_{\xi\in\mathbb{R}}\Big|\frac{e^{(1-x)(\Phi(\xi)-i\Psi(\xi))}-\min\{e^{(1-x)(\Phi(\xi)-i\Psi(\xi))},\mu(x)e^{i(1-x)\Psi(\xi)}\}}{e^{\Phi(\xi)-i\Psi(\xi)}}\Big|E \\ &\le E\sup_{\xi\in\mathbb{R},e^{(1-x)\Phi(\xi)}>\mu(x)}\Big|\frac{e^{(1-x)\Phi(\xi)}-\mu(x)}{e^{\Phi(\xi)}}\Big| \\ &=E\sup_{\xi\in\mathbb{R},e^{(1-x)\Phi(\xi)}>\mu(x)}\frac{e^{(1-x)\Phi(\xi)}-\mu(x)}{e^{\Phi(\xi)}}.\end{aligned} \tag{4.8}$$

Denote $\gamma:=\Phi(\xi)$ and let

$$G(\gamma)=\frac{e^{(1-x)\gamma}-\mu(x)}{e^{\gamma}}.$$

Suppose γ^* satisfies $G'(\gamma^*)=0$, by a simple calculation, we obtain

$$\gamma^*=\frac{1}{1-x}\ln\Big(\frac{1}{x}\mu(x)\Big),$$

then we have

$$I_2\le EG(\gamma^*)=E\frac{(\frac{1}{x}-1)\mu(x)}{(\frac{1}{x}\mu(x))^{\frac{1}{1-x}}}. \tag{4.9}$$

Combining (4.6), (4.7) and (4.9), we obtain

$$\|u_\mu^\delta(x,t)-u(x,t)\|\le I_1+I_2\le\delta\mu(x)+E\frac{(\frac{1}{x}-1)\mu(x)}{(\frac{1}{x}\mu(x))^{\frac{1}{1-x}}}.$$

Choosing the regularization parameter $\mu(x)$ by

$$\mu(x)=x\Big(\frac{E}{\delta}\Big)^{1-x},$$

we then obtain the following convergence estimate

$$\|u_\mu^\delta(x,t)-u(x,t)\|\le\delta^x E^{1-x}.$$

The proof of the theorem has been completed. ■

Remark 4.1. *When $x = 0$, the error estimate in **Theorem** 4.1 is only bounded instead of convergence. In order to obtain the convergent error estimate between the exact solution and the regularization solution at $x = 0$, a stronger priori hypothesis must be introduced. Therefore, for $x = 0$, there is the following theorem.*

Theorem 4.2. *Suppose that $u_\mu^\delta(x,t)$ given by (4.3) is the regularization solution of the exact solution (2.5). Let $p > 0$ and let the assumption (2.1) and (2.6) be satisfied. If we choose*

$$\mu = \frac{p}{p+2}\Big(\frac{E}{\delta}\Big)^{\frac{2}{p+2}}, \tag{4.10}$$

then for $x = 0$, we obtain the following error estimate

$$\|u_\mu^\delta(0,t) - u(0,t)\| \le \delta^{\frac{p}{p+2}} E^{\frac{2}{p+2}}. \tag{4.11}$$

Proof. Due to the Parseval's identity and the triangle inequality, we can obtain

$$\begin{aligned}
\|u_\mu^\delta(0,t) - u(0,t)\| &= \|\hat{u}_\mu^\delta(0,\xi) - \hat{u}(0,\xi)\| \\
&\le \|\hat{u}_\mu^\delta(0,\xi) - \hat{u}_\mu(0,\xi)\| + \|\hat{u}_\mu(0,\xi) - \hat{u}(0,\xi)\| \\
&= \|k_\mu(0,\xi)\hat{f}^\delta - k_\mu(0,\xi)\hat{f}\| + \|k_\mu(0,\xi)\hat{f} - \hat{u}(0,\xi)\| \\
&= I_3 + I_4,
\end{aligned} \tag{4.12}$$

where

$$I_3 = \|k_\mu(0,\xi)\hat{f}^\delta - k_\mu(0,\xi)\hat{f}\| = \|k_\mu(0,\xi)(\hat{f}^\delta - \hat{f})\| \le \sup_{\xi\in\mathbb{R}} |k_\mu(0,\xi)|\delta \le \delta\mu, \tag{4.13}$$

and

$$\begin{aligned}
I_4 &= \Big\|\frac{k_\mu(0,\xi) - e^{\theta(\xi)}}{e^{\theta(\xi)}}\hat{u}(0,\xi)\Big\| \\
&= \Big\|\frac{e^{\Phi(\xi)+i\Psi(\xi)} - k_\mu(0,\xi)}{e^{\Phi(\xi)+i\Psi(\xi)}} e^{-\frac{p}{2}\Phi(\xi)} e^{\frac{p}{2}\Phi(\xi)}\hat{u}(0,\xi)\Big\| \\
&\le \sup_{\xi\in\mathbb{R}}\Big|\frac{e^{\Phi(\xi)+i\Psi(\xi)} - \min\{e^{\Phi(\xi)+i\Psi(\xi)}, \mu e^{i\Psi(\xi)}\}}{e^{\Phi(\xi)+i\Psi(\xi)}} e^{-\frac{p}{2}\Phi(\xi)}\Big| E \\
&\le E \sup_{\xi\in\mathbb{R}, e^{\Phi(\xi)}>\mu}\Big|\frac{e^{\Phi(\xi)} - \mu}{e^{\Phi(\xi)}} e^{-\frac{p}{2}\Phi(\xi)}\Big| \\
&= E \sup_{\xi\in\mathbb{R}, e^{\Phi(\xi)}>\mu}\frac{e^{\Phi(\xi)} - \mu}{e^{(\frac{p}{2}+1)\Phi(\xi)}}.
\end{aligned} \tag{4.14}$$

Denote $\gamma := \Phi(\xi)$ and let

$$H(\gamma) = \frac{e^\gamma - \mu}{e^{(\frac{p}{2}+1)\gamma}}.$$

Suppose $\gamma^\star$ satisfies $H^{'}(\gamma^\star) = 0$, then we obtain

$$\gamma^\star = \ln\Big(\frac{p+2}{p}\mu\Big),$$

then

$$I_4 \le EH(\gamma^\star) = E\frac{(\frac{p+2}{p}-1)\mu}{(\frac{p+2}{p}\mu)^{\frac{p+2}{2}}}. \tag{4.15}$$

Combining (4.10), (4.12), (4.13) and (4.15), we obtain the convergence estimate

$$\|u_\mu^\delta(0,t)-u(0,t)\| \le I_3+I_4 \le \delta^{\frac{p}{p+2}}E^{\frac{2}{p+2}}.$$

We have completed the proof of theorem. ■

4.2 The error estimate with a posteriori parameter choice

In this section, we consider a posteriori regularization parameter choice rule. The most general a posteriori rule is the Morozov's discrepancy principle [48] that is used to determine the regularization parameter $\mu(x)$.

Let $\tau>1$ be given a fixed constant. According to Morozov's discrepancy principle, we use the regularization parameter $\mu(x)$ as the solution of the equation

$$\|e^{-(1-x)\theta(\xi)}k_\mu(x,\xi)\hat{f}^\delta-\hat{f}^\delta\| = \tau\delta,\quad 0\le x<1. \tag{4.16}$$

Let $\mathcal{K}_\mu = e^{-(1-x)\theta(\xi)}k_\mu(x,\xi)-1$, we have the following lemma.

Lemma 4.1. *Let $\omega(\mu)=\|\mathcal{K}_\mu\hat{f}^\delta\| = \|e^{-(1-x)\theta(\xi)}k_\mu(x,\xi)\hat{f}^\delta-\hat{f}^\delta\|$, then we have the following results*
(a) $\omega(\mu)$ is a continuous function;
(b) $\lim_{\mu\to1}\omega(\mu)=\|(e^{-(1-x)\Phi(\xi)}-1)\hat{f}^\delta\|$;
(c) $\lim_{\mu\to+\infty}\omega(\mu)=0$;
(d) $\omega(\mu)$ is a strictly decreasing function for any $\mu\in(1,+\infty)$.

Remark 4.2. *The proof of **Lemma** 4.1 is obvious, and we omitted it here. From **Lemma** 4.1, we know that if $0<\tau\delta<\|(e^{-(1-x)\Phi(\xi)}-1)\hat{f}^\delta\|$, the equation (4.16) exists a unique solution.*

Lemma 4.2. *Let $p=0$ and let the assumption (2.1) and (2.6) be satisfied. If $\mu(x)$ is the solution of equation (4.16), then for every $x\in(0,1)$, $\mu(x)$ satisfies the following inequality*

$$\mu(x) \le \Big(\frac{E}{(\tau-1)\delta}\Big)^{1-x}. \tag{4.17}$$

Proof. First we know $|\mathcal{K}_\mu|\le1$. Due to the triangle inequality and (4.16) we have

$$\tau\delta = \|\mathcal{K}_\mu\hat{f}^\delta\| \le \|\mathcal{K}_\mu(\hat{f}^\delta-\hat{f})\| + \|\mathcal{K}_\mu\hat{f}\| \le \delta + \|\mathcal{K}_\mu\hat{f}\|. \tag{4.18}$$

For the right side of the upper formula (4.18), we can obtain

$$
\begin{aligned}
\|\mathcal{K}_\mu \hat{f}\| &= \|(e^{-(1-x)\theta(\xi)}k_\mu(x,\xi)-1)e^{-\theta(\xi)}\hat{u}(0,\xi)\| \\
&= \Big\|\frac{1-e^{-(1-x)\theta(\xi)}k_\mu(x,\xi)}{e^{\theta(\xi)}}\hat{u}(0,\xi)\Big\| \\
&= \Big\|\frac{e^{(1-x)\theta(\xi)}-k_\mu(x,\xi)}{e^{(2-x)\theta(\xi)}}\hat{u}(0,\xi)\Big\| \\
&\le \sup_{\xi\in\mathbb{R}}\Big|\frac{e^{(1-x)\theta(\xi)}-k_\mu(x,\xi)}{e^{(2-x)\theta(\xi)}}\Big|E \\
&\le E \sup_{\xi\in\mathbb{R},e^{(1-x)\Phi(\xi)}>\mu(x)} \frac{e^{(1-x)\Phi(\xi)}-\mu(x)}{e^{(2-x)\Phi(\xi)}} \\
&= E \sup_{\xi\in\mathbb{R},e^{(1-x)\Phi(\xi)}>\mu(x)} \frac{e^{(1-x)\Phi(\xi)}-\mu(x)}{e^{(1-x)\Phi(\xi)}}e^{-\Phi(\xi)} \\
&\le E \sup_{\xi\in\mathbb{R},e^{(1-x)\Phi(\xi)}>\mu(x)} e^{-\Phi(\xi)}.
\end{aligned}
\tag{4.19}
$$

Note that $e^{(1-x)\Phi(\xi)} > \mu(x)$, we have $e^{-\Phi(\xi)} \le \mu(x)^{-\frac{1}{1-x}}$, therefore we can obtain

$$
\|\mathcal{K}_\mu \hat{f}\| \le E \sup_{\xi\in\mathbb{R},e^{(1-x)\Phi(\xi)}>\mu(x)} e^{-\Phi(\xi)} \le E\mu(x)^{-\frac{1}{1-x}}. \tag{4.20}
$$

Combining (4.18) and (4.20), we have

$$
(\tau-1)\delta \le E\mu(x)^{-\frac{1}{1-x}}, \tag{4.21}
$$

i.e.,

$$
\mu(x) \le \Big(\frac{E}{(\tau-1)\delta}\Big)^{1-x}.
$$

The proof of lemma has been completed. ∎

Theorem 4.3. *Suppose that $u_\mu^\delta(x,t)$ given by (4.3) is the regularization solution of the exact solution (2.5). Let $p=0$ and let the assumption (2.1) and (2.6) be satisfied. Taking the solution of equation (4.16) as the regularization parameter, then for every $x\in(0,1)$, we obtain the following error estimate*

$$
\|u_\mu^\delta(x,t)-u(x,t)\| \le C_1\delta^x E^{1-x}, \tag{4.22}
$$

where $C_1=(\tau-1)^{x-1}+(2\tau^2+2)^{\frac{x}{2}}$ is positive constant.

Proof. Due to the Parseval's identity and the triangle inequality, we have

$$
\begin{aligned}
\|u_\mu^\delta(x,t)-u(x,t)\| &= \|\hat{u}_\mu^\delta(x,\xi)-\hat{u}(x,\xi)\| \\
&\le \|\hat{u}_\mu^\delta(x,\xi)-\hat{u}_\mu(x,\xi)\| + \|\hat{u}_\mu(x,\xi)-\hat{u}(x,\xi)\| \\
&= \delta\mu(x) + \|\hat{u}_\mu(x,\xi)-\hat{u}(x,\xi)\|.
\end{aligned}
\tag{4.23}
$$

According to **Lemma** 4.2, we obtain

$$
\delta\mu(x) \le (\tau-1)^{x-1}\delta^x E^{1-x}. \tag{4.24}
$$

Due to the *Hölder* inequality, for the right side of the upper formula (4.23), we have

$$
\begin{aligned}
\|\hat{u}_\mu(x,\xi)-\hat{u}(x,\xi)\|^2 &= \|(k_\mu(x,\xi)-e^{(1-x)\theta(\xi)})\hat{f}\|^2 \\
&= \|(k_\mu(x,\xi)-e^{(1-x)\theta(\xi)})e^{-\theta(\xi)}\hat{u}(0,\xi)\|^2 \\
&= \|\frac{k_\mu(x,\xi)-e^{(1-x)\theta(\xi)}}{e^{(1-x)\theta(\xi)}}|\hat{f}|^x|\hat{u}(0,\xi)|^{1-x}\|^2 \\
&= \|(e^{-(1-x)\theta(\xi)}k_\mu(x,\xi)-1)|\hat{f}|^x|\hat{u}(0,\xi)|^{1-x}\|^2 \\
&= \|\mathcal{K}_\mu|\hat{f}|^x|\hat{u}(0,\xi)|^{1-x}\|^2 \\
&= \||\mathcal{K}_\mu\hat{f}|^x|\mathcal{K}_\mu\hat{u}(0,\xi)|^{1-x}\|^2 \\
&= \int_{-\infty}^{+\infty}|\mathcal{K}_\mu\hat{f}|^{2x}|\mathcal{K}_\mu\hat{u}(0,\xi)|^{2(1-x)}d\xi \\
&\le \Big(\int_{-\infty}^{+\infty}|\mathcal{K}_\mu\hat{f}|^2d\xi\Big)^x\Big(\int_{-\infty}^{+\infty}|\mathcal{K}_\mu\hat{u}(0,\xi)|^2d\xi\Big)^{1-x} \\
&\le 2^x\Big(\int_{-\infty}^{+\infty}|\mathcal{K}_\mu|^2(|\hat{f}-\hat{f}^\delta|^2+|\hat{f}^\delta|^2)d\xi\Big)^xE^{2(1-x)} \\
&= 2^x(\|\mathcal{K}_\mu(\hat{f}-\hat{f}^\delta)\|^2+\|\mathcal{K}_\mu\hat{f}^\delta\|^2)^xE^{2(1-x)} \\
&\le (2\tau^2+2)^x\delta^{2x}E^{2(1-x)},
\end{aligned}
$$

therefore, we obtain

$$\|\hat{u}_\mu(x,\xi)-\hat{u}(x,\xi)\| \le (2\tau^2+2)^{\frac{x}{2}}\delta^xE^{1-x}. \tag{4.25}$$

Combining (4.23), (4.24) and (4.25), we have

$$\|u_\mu^\delta(x,t)-u(x,t)\| \le C_1\delta^xE^{1-x},$$

where $C_1=(\tau-1)^{x-1}+(2\tau^2+2)^{\frac{x}{2}}$.
The proof of theorem is completed. ■

Remark 4.3. *When $x=0$, the error estimate in **Theorem** 4.3 is only bound, not convergence. Therefore, for $x=0$, we give the following lemma.*

Lemma 4.3. *Let $p>0$ and let the assumption (2.1) and (2.6) be satisfied. If μ is the solution of equation (4.16), then for $x=0$, μ satisfies the following inequality*

$$\mu \le \Big(\frac{E}{(\tau-1)\delta}\Big)^{\frac{2}{p+2}}. \tag{4.26}$$

Proof. Let $\mathcal{K}_\mu^0=e^{-\theta(\xi)}k_\mu(0,\xi)-1$. Due to the triangle inequality and (4.16), we have

$$\tau\delta=\|\mathcal{K}_\mu^0\hat{f}^\delta\| \le \|\mathcal{K}_\mu^0(\hat{f}^\delta-\hat{f})\|+\|\mathcal{K}_\mu^0\hat{f}\| \le \delta+\|\mathcal{K}_\mu^0\hat{f}\|, \tag{4.27}$$

where

$$
\begin{aligned}
\|\mathcal{K}_\mu^0 \hat{f}\| &= \|(e^{-\theta(\xi)} k_\mu(0,\xi) - 1) e^{-\theta(\xi)} \hat{u}(0,\xi)\| \\
&= \Big\| \frac{1 - e^{-\theta(\xi)} k_\mu(0,\xi)}{e^{\theta(\xi)}} e^{-\frac{p}{2}\Phi(\xi)} e^{\frac{p}{2}\Phi(\xi)} \hat{u}(0,\xi) \Big\| \\
&= \Big\| \frac{e^{\theta(\xi)} - k_\mu(0,\xi)}{e^{2\theta(\xi)}} e^{-\frac{p}{2}\Phi(\xi)} e^{\frac{p}{2}\Phi(\xi)} \hat{u}(0,\xi) \Big\| \\
&\le \sup_{\xi\in\mathbb{R}} \Big| \frac{e^{\theta(\xi)} - k_\mu(0,\xi)}{e^{2\theta(\xi)}} e^{-\frac{p}{2}\Phi(\xi)} \Big| E \\
&\le E \sup_{\xi\in\mathbb{R}, e^{\Phi(\xi)} > \mu} \Big| \frac{e^{\Phi(\xi)} - \mu}{e^{\Phi(\xi)}} e^{-(\frac{p}{2}+1)\Phi(\xi)} \Big| \\
&\le E \sup_{\xi\in\mathbb{R}, e^{\Phi(\xi)} > \mu} e^{-(\frac{p}{2}+1)\Phi(\xi)}.
\end{aligned}
$$

Similar to the proof of **Lemma** 4.2, we obtain

$$
\|\mathcal{K}_\mu^0 \hat{f}\| \le E \sup_{\xi\in\mathbb{R}, e^{\Phi(\xi)} > \mu} e^{-(\frac{p}{2}+1)\Phi(\xi)} \le E\mu^{-\frac{p+2}{2}}. \tag{4.28}
$$

Combining (4.27) and (4.28), we obtain

$$
\mu \le \Big(\frac{E}{(\tau-1)\delta} \Big)^{\frac{2}{p+2}}.
$$

The proof has been completed. ■

Theorem 4.4. *Suppose that $u_\mu^\delta(x,t)$ given by (4.3) is the regularization solution of the exact solution (2.5). Let $p > 0$ and let the assumption (2.1) and (2.6) be satisfied. Taking the solution of equation (4.16) as the regularization parameter, then for $x = 0$, we have the following error estimate*

$$
\|u_\mu^\delta(0,t) - u(0,t)\| \le C_2 \delta^{\frac{p}{p+2}} E^{\frac{2}{p+2}}, \tag{4.29}
$$

where $C_2 = (\tau-1)^{-\frac{2}{p+2}} + (2\tau^2+2)^{\frac{p}{2(p+2)}}$ is positive constant.

Proof. Due to the Parseval's identity and the triangle inequality, we have

$$
\begin{aligned}
\|u_\mu^\delta(0,t) - u(0,t)\| &= \|\hat{u}_\mu^\delta(0,\xi) - \hat{u}(0,\xi)\| \\
&\le \|\hat{u}_\mu^\delta(0,\xi) - \hat{u}_\mu(0,\xi)\| + \|\hat{u}_\mu(0,\xi) - \hat{u}(0,\xi)\| \\
&\le \delta\mu + \|\hat{u}_\mu(0,\xi) - \hat{u}(0,\xi)\|.
\end{aligned} \tag{4.30}
$$

Form **Lemma** 4.3, we obtain

$$
\delta\mu \le (\tau-1)^{-\frac{2}{p+2}} \delta^{\frac{p}{p+2}} E^{\frac{2}{p+2}}. \tag{4.31}
$$

According to the *Hölder* inequality, we have

$$\begin{aligned}
\|\hat{u}_\mu(0,\xi)-\hat{u}(0,\xi)\|^2 &= \|(k_\mu(0,\xi)-e^{\theta(\xi)})\hat{f}\|^2 \\
&= \|(k_\mu(0,\xi)-e^{\theta(\xi)})e^{-\theta(\xi)}\hat{u}(0,\xi)\|^2 \\
&= \|\frac{k_\mu(0,\xi)-e^{\theta(\xi)}}{e^{\theta(\xi)}}|\hat{f}|^{\frac{p}{p+2}}|e^{\frac{p}{2}\Phi(\xi)}\hat{u}(0,\xi)|^{\frac{2}{p+2}}\|^2 \\
&= \|(e^{-\theta(\xi)}k_\mu(0,\xi)-1)|\hat{f}|^{\frac{p}{p+2}}|e^{\frac{p}{2}\Phi(\xi)}\hat{u}(0,\xi)|^{\frac{2}{p+2}}\|^2 \\
&= \||\mathcal{K}_\mu^0\hat{f}|^{\frac{p}{p+2}}|\mathcal{K}_\mu^0 e^{\frac{p}{2}\Phi(\xi)}\hat{u}(0,\xi)|^{\frac{2}{p+2}}\|^2 \\
&= \int_{-\infty}^{+\infty}|\mathcal{K}_\mu^0\hat{f}|^{\frac{2p}{p+2}}|\mathcal{K}_\mu^0 e^{\frac{p}{2}\Phi(\xi)}\hat{u}(0,\xi)|^{\frac{4}{p+2}}d\xi \\
&\le \Big(\int_{-\infty}^{+\infty}|\mathcal{K}_\mu^0\hat{f}|^2 d\xi\Big)^{\frac{p}{p+2}}\Big(\int_{-\infty}^{+\infty}|\mathcal{K}_\mu^0 e^{\frac{p}{2}\Phi(\xi)}\hat{u}(0,\xi)|^2 d\xi\Big)^{\frac{2}{p+2}} \\
&\le 2^{\frac{p}{p+2}}\Big(\int_{-\infty}^{+\infty}|\mathcal{K}_\mu^0|^2(|\hat{f}-\hat{f}^\delta|^2+|\hat{f}^\delta|^2)d\xi\Big)^{\frac{p}{p+2}}E^{\frac{4}{p+2}} \\
&= 2^{\frac{p}{p+2}}(\|\mathcal{K}_\mu^0(\hat{f}-\hat{f}^\delta)\|^2+\|\mathcal{K}_\mu^0\hat{f}^\delta\|^2)^{\frac{p}{p+2}}E^{\frac{4}{p+2}} \\
&\le (2\tau^2+2)^{\frac{p}{p+2}}\delta^{\frac{2p}{p+2}}E^{\frac{4}{p+2}},
\end{aligned}$$

then we have

$$\|\hat{u}_\mu(x,\xi)-\hat{u}(x,\xi)\| \le (2\tau^2+2)^{\frac{p}{2(p+2)}}\delta^{\frac{p}{p+2}}E^{\frac{2}{p+2}}. \tag{4.32}$$

Combining (4.30), (4.31) and (4.32), we obtain

$$\|u_\mu^\delta(x,t)-u(x,t)\| \le C_2\delta^x E^{1-x},$$

where $C_2=(\tau-1)^{-\frac{2}{p+2}}+(2\tau^2+2)^{\frac{p}{2(p+2)}}$.
The proof of theorem has been completed. ■

5 Analysis of optimal approximation

In this section, we will analyze the optimality of the error estimates obtained by this regularization method.

Table 1: Error estimation coefficient value for different x.

Parameter selection rules	the priori	the posteriori
$0<x<1$, $p=0$	1	$(\tau-1)^{x-1}+(2\tau^2+2)^{\frac{x}{2}}$
$x=0$, $p>0$	1	$(\tau-1)^{-\frac{2}{p+2}}+(2\tau^2+2)^{\frac{p}{2(p+2)}}$

For $0<x<1$, we choose $\|u(0,t)\|_{M^0(\mathbb{R})}=\|u(0,t)\|_{L^2(\mathbb{R})}=\Big(\int_{-\infty}^{+\infty}|\hat{u}(0,\xi)|^2d\xi\Big)^{\frac{1}{2}}\le E$ as a priori bound, i.e., let $p=0$ in (2.6). From **Table** 1 and **Theorem** 3.2, we know that the priori error estimate obtained by using a modified kernel method is optimal and the posteriori error estimate is order-optimal. When $x = 0$, we choose $\|u(0,t)\|_{M^p(\mathbb{R})} = \Big(\int_{-\infty}^{+\infty} e^{p\Phi(\xi)}|\hat{u}(0,\xi)|^2 d\xi\Big)^{\frac{1}{2}} \le E$ as a priori bound, where $p > 0$. According to **Theorem** 3.2 and **Table** 1, we obtain that the priori error estimate is optimal and the posteriori error estimate is order-optimal.

From the above analysis, under given priori bound (2.6), the modified kernel method is effective. Next, we will give some numerical examples to verify the effectiveness of this method.

6 Numerical examples

In this section, we give numerical examples to illustrate the efficiency and stability of the method.

It is a well-posed problem to compute the function $u(1,t) = f(t)$ by solving a direct problem when the initial data $u(0,t) = g(t)$ of the problem (1.1) at $x = 0$ is known. Therefore, its solution at $x = 1$ is given by

$$f(t) = u(1,t) = \frac{1}{\sqrt{2\pi}} \int_{-\infty}^{+\infty} e^{-\theta(\xi)} \hat{g}(\xi) e^{i\xi t} d\xi. \tag{6.1}$$

In the numerical implementation, we give the data $g(t)$ of $N+1$ equidistant grid points on the domain $[0,T]$ and perform the discrete Fourier transform. Then the data $f(t)$ is obtained by (6.1) and the inverse discrete Fourier transform is performed to generate the noise data $\hat{f}$ as follows:

$$\hat{f}^\delta = \hat{f} + \varepsilon \cdot randn(size(\hat{f})),$$

where ε represents the relative error level. This absolute error level δ is expressed as

$$\delta = \sqrt{\frac{1}{N+1} \sum_{i=1}^{N+1} (\hat{f}_i - \hat{f}_i^\delta)^2}.$$

To see the accuracy of numerical solutions, we compute the relative root mean square errors by

$$\epsilon(u) = \Big(\sum_{i=1}^{n} (u_\mu^\delta(x,t_i) - u(x,t_i))^2 \Big/ \sum_{i=1}^{n} u(x,t_i)^2 \Big)^{1/2},$$

where n is the total number of test points.

We know that the priori regularization parameters are based on the smoothness condition of the exact solution, which is actually difficult to give in advance. Therefore, the following examples are based on the posteriori regularization parameters to verify the effectiveness of the regularization method.

Choosing $N = 100$, $T = 2$, we give the following three examples.

Example 1. Consider a smooth function $u(0,t) := g(t) = e^{-2\pi i t} - 1$.

Example 2. Consider a piecewise smooth function

$$u(0,t) := g(t) = \begin{cases} (\pi + i)t, & 0 \le t < 1, \\ (\pi + i)(2 - t), & 1 \le t \le 2. \end{cases}$$

Example 3. Consider a non-smooth function

$$u(0,t) := g(t) = \begin{cases} 0, & 0 \le t < \frac{1}{2}, \\ 1-i, & \frac{1}{2} \le t < 1, \\ i-1, & 1 \le t < \frac{3}{2}, \\ 0, & \frac{3}{2} \le t \le 2. \end{cases}$$

Table 2: The relative root mean square errors of real parts between the exact and approximate solutions of Example 1 for various values of x and α.

x		0	0.1	0.3	0.5	0.7	0.9
$\alpha = 0.1$	$\varepsilon = 0.1$	4.0195	0.8544	0.6285	0.4372	0.2651	0.0927
$\epsilon(u)$	$\varepsilon = 0.01$	4.0162	0.8528	0.6275	0.4371	0.2645	0.0918
	$\varepsilon = 0.001$	4.0152	0.8526	0.6274	0.4370	0.2644	0.0917
$\alpha = 0.5$	$\varepsilon = 0.1$	5.0843	0.7553	0.6390	0.4943	0.3187	0.1155
$\epsilon(u)$	$\varepsilon = 0.01$	5.0777	0.7550	0.6388	0.4936	0.3185	0.1133
	$\varepsilon = 0.001$	5.0776	0.7550	0.6387	0.4935	0.3184	0.1133
$\alpha = 0.8$	$\varepsilon = 0.1$	5.1256	0.8383	0.7376	0.5967	0.4037	0.1524
$\epsilon(u)$	$\varepsilon = 0.01$	5.1203	0.8380	0.7374	0.5956	0.4031	0.1509
	$\varepsilon = 0.001$	5.1201	0.8380	0.7372	0.5955	0.4030	0.1508
$\alpha = 0.9$	$\varepsilon = 0.1$	5.0314	0.8526	0.7571	0.6189	0.4247	0.1619
$\epsilon(u)$	$\varepsilon = 0.01$	5.0281	0.8525	0.7569	0.6185	0.4244	0.1613
	$\varepsilon = 0.001$	5.0281	0.8524	0.7568	0.6184	0.4243	0.1613

Figure 1-8 show the real parts and the imaginary parts of the exact solution and its approximation solution under the modified kernel method for **Example 1** with $\alpha = 0.1, 0.5, 0.8, 0.9$ by taking $\varepsilon = 0.1, 0.01, 0.001$. **Table 2** and **Table 3** show the relative root mean square errors of the real parts and the imaginary parts between the exact and approximate solutions of **Example 1** with various values $x = 0, 0.1, 0.3, 0.5, 0.7, 0.9$ and $\alpha = 0.1, 0.5, 0.8, 0.9$.

Figure 9-16 show the real parts and the imaginary parts of the exact solution and its approximation solution under the modified kernel method for **Example 2** with $\alpha = 0.1, 0.5, 0.8, 0.9$ by taking $\varepsilon = 0.1, 0.01, 0.001$. **Table 4** and **Table 5** show the relative root mean square errors of the real parts and the imaginary parts between the exact and approximate solutions of **Example 2** with various values $x = 0, 0.1, 0.3, 0.5, 0.7, 0.9$ and $\alpha = 0.1, 0.5, 0.8, 0.9$.

Figure 17-24 show the real parts and the imaginary parts of the exact solution and its approximation solution under the modified kernel method for **Example 3** with $\alpha = 0.1, 0.5, 0.8, 0.9$ by taking $\varepsilon = 0.1, 0.01, 0.001$. **Table 6** and **Table 7** show the relative root mean square errors of the real parts and the imaginary parts between the exact and approximate solutions of **Example 3** with various values $x = 0, 0.1, 0.3, 0.5, 0.7, 0.9$ and $\alpha = 0.1, 0.5, 0.8, 0.9$.

Table 3: The relative root mean square errors of imaginary parts between the exact and approximate solutions of Example 1 for various values of x and α.

x		0	0.1	0.3	0.5	0.7	0.9
$\alpha = 0.1$	$\varepsilon = 0.1$	3.2720	0.9775	0.8962	0.7647	0.5568	0.2290
$\epsilon(u)$	$\varepsilon = 0.01$	3.2541	0.9767	0.8957	0.7641	0.5565	0.2288
	$\varepsilon = 0.001$	3.2540	0.9767	0.8957	0.7641	0.5565	0.2288
$\alpha = 0.5$	$\varepsilon = 0.1$	2.9031	1.0925	1.0423	0.9297	0.7072	0.3040
$\epsilon(u)$	$\varepsilon = 0.01$	2.8993	1.0917	1.0420	0.9292	0.7068	0.3038
	$\varepsilon = 0.001$	2.8987	1.0917	1.0419	0.9288	0.7067	0.3037
$\alpha = 0.8$	$\varepsilon = 0.1$	4.3805	1.0682	1.0263	0.9246	0.7137	0.3119
$\epsilon(u)$	$\varepsilon = 0.01$	4.3763	1.0678	1.0259	0.9239	0.7128	0.3116
	$\varepsilon = 0.001$	4.3753	1.0678	1.0259	0.9239	0.7128	0.3116
$\alpha = 0.9$	$\varepsilon = 0.1$	4.7722	1.0209	0.9758	0.8765	0.6767	0.2967
$\epsilon(u)$	$\varepsilon = 0.01$	4.7640	1.0205	0.9756	0.8761	0.6762	0.2965
	$\varepsilon = 0.001$	4.7631	1.0204	0.9756	0.8761	0.6762	0.2965

Table 4: The relative root mean square errors of real parts between the exact and approximate solutions of Example 2 for various values of x and α.

x		0	0.1	0.3	0.5	0.7	0.9
$\alpha = 0.1$	$\varepsilon = 0.1$	2.9848	0.6230	0.5351	0.4250	0.2849	0.1104
$\epsilon(u)$	$\varepsilon = 0.01$	2.9776	0.6221	0.5346	0.4236	0.2828	0.1051
	$\varepsilon = 0.001$	2.9772	0.6221	0.5345	0.4235	0.2827	0.1050
$\alpha = 0.5$	$\varepsilon = 0.1$	3.6806	0.7210	0.6229	0.4579	0.3068	0.1147
$\epsilon(u)$	$\varepsilon = 0.01$	3.6723	0.7200	0.6223	0.4569	0.3043	0.1130
	$\varepsilon = 0.001$	3.6721	0.7199	0.6222	0.4568	0.3043	0.1129
$\alpha = 0.8$	$\varepsilon = 0.1$	3.9022	0.7324	0.6414	0.5190	0.3549	0.1375
$\epsilon(u)$	$\varepsilon = 0.01$	3.8986	0.7321	0.6406	0.5181	0.3545	0.1356
	$\varepsilon = 0.001$	3.8982	0.7321	0.6405	0.5181	0.3544	0.1356
$\alpha = 0.9$	$\varepsilon = 0.1$	3.9983	0.7481	0.6580	0.5357	0.3689	0.1428
$\epsilon(u)$	$\varepsilon = 0.01$	3.9916	0.7478	0.6576	0.5349	0.3685	0.1422
	$\varepsilon = 0.001$	3.9915	0.7478	0.6575	0.5349	0.3684	0.1421

Table 5: The relative root mean square errors of imaginary parts between the exact and approximate solutions of Example 2 for various values of x and α.

x		0	0.1	0.3	0.5	0.7	0.9
$\alpha = 0.1$	$\varepsilon = 0.1$	10.9124	0.5150	0.4045	0.2918	0.1176	0.0604
$\epsilon(u)$	$\varepsilon = 0.01$	10.9066	0.5147	0.4042	0.2917	0.1175	0.0604
	$\varepsilon = 0.001$	10.9066	0.5147	0.4042	0.2917	0.1175	0.0604
$\alpha = 0.5$	$\varepsilon = 0.1$	13.4920	0.6434	0.5433	0.4249	0.2795	0.1025
$\epsilon(u)$	$\varepsilon = 0.01$	13.4898	0.6433	0.5432	0.4248	0.2795	0.1025
	$\varepsilon = 0.001$	13.4897	0.6433	0.5431	0.4248	0.2795	0.1025
$\alpha = 0.8$	$\varepsilon = 0.1$	15.0883	0.7072	0.6136	0.4913	0.3322	0.1254
$\epsilon(u)$	$\varepsilon = 0.01$	15.0860	0.7071	0.6135	0.4912	0.3321	0.1254
	$\varepsilon = 0.001$	15.0859	0.7071	0.6135	0.4912	0.3321	0.1254
$\alpha = 0.9$	$\varepsilon = 0.1$	15.1149	0.7297	0.6373	0.5143	0.3508	0.1337
$\epsilon(u)$	$\varepsilon = 0.01$	15.1143	0.7296	0.6372	0.5143	0.3507	0.1337
	$\varepsilon = 0.001$	15.1142	0.7296	0.6371	0.5142	0.3507	0.1337

Table 6: The relative root mean square errors of real parts between the exact and approximate solutions of Example 3 for various values of x and α.

x		0	0.1	0.3	0.5	0.7	0.9
$\alpha = 0.1$	$\varepsilon = 0.1$	4.2159	1.1307	1.0848	0.9390	0.6604	0.2456
$\epsilon(u)$	$\varepsilon = 0.01$	4.2090	1.1306	1.0846	0.9389	0.6587	0.2441
	$\varepsilon = 0.001$	4.2087	1.1305	1.0845	0.9389	0.6586	0.2440
$\alpha = 0.5$	$\varepsilon = 0.1$	4.3197	1.0781	1.0307	0.9039	0.6581	0.2608
$\epsilon(u)$	$\varepsilon = 0.01$	4.3167	1.0780	1.0306	0.9036	0.6577	0.2603
	$\varepsilon = 0.001$	4.3164	1.0780	1.0306	0.9036	0.6576	0.2602
$\alpha = 0.8$	$\varepsilon = 0.1$	4.6048	1.0743	1.0447	0.9363	0.7003	0.2874
$\epsilon(u)$	$\varepsilon = 0.01$	4.6034	1.0741	1.0446	0.9362	0.7000	0.2867
	$\varepsilon = 0.001$	4.6032	1.0741	1.0446	0.9361	0.6999	0.2866
$\alpha = 0.9$	$\varepsilon = 0.1$	4.6601	1.0761	1.0539	0.9525	0.7192	0.2986
$\epsilon(u)$	$\varepsilon = 0.01$	4.6563	1.0759	1.0538	0.9524	0.7187	0.2975
	$\varepsilon = 0.001$	4.6562	1.0748	1.0537	0.9524	0.7186	0.2974

Table 7: The relative root mean square errors of imaginary parts between the exact and approximate solutions of Example 3 for various values of x and α.

x		0	0.1	0.3	0.5	0.7	0.9
$\alpha = 0.1$	$\varepsilon = 0.05$	3.5342	1.0440	0.9220	0.7499	0.5362	0.2300
$\epsilon(u)$	$\varepsilon = 0.01$	3.5301	1.0435	0.9215	0.7490	0.5349	0.2294
	$\varepsilon = 0.001$	3.5297	1.0434	0.9214	0.7489	0.5348	0.2294
$\alpha = 0.5$	$\varepsilon = 0.05$	4.8627	1.0460	0.9890	0.8732	0.6627	0.2873
$\epsilon(u)$	$\varepsilon = 0.01$	4.8602	1.0458	0.9888	0.8724	0.6622	0.2870
	$\varepsilon = 0.001$	4.8598	1.0458	0.9888	0.8723	0.6621	0.2870
$\alpha = 0.8$	$\varepsilon = 0.05$	5.2484	1.0736	1.0544	0.9698	0.7631	0.3386
$\epsilon(u)$	$\varepsilon = 0.01$	5.2442	1.0736	1.0540	0.9692	0.7626	0.3383
	$\varepsilon = 0.001$	5.2436	1.0736	1.0540	0.9692	0.7626	0.3383
$\alpha = 0.9$	$\varepsilon = 0.05$	5.3040	1.0788	1.0711	0.9978	0.7946	0.3551
$\epsilon(u)$	$\varepsilon = 0.01$	5.3036	1.0787	1.0708	0.9972	0.7936	0.3548
	$\varepsilon = 0.001$	5.3028	1.0787	1.0707	0.9971	0.7935	0.3547

According to the above three examples, it can be proved that for a given x and ε, $\epsilon(u)$ increases with the increase of α, i.e., the larger α, the more serious the problem is. And for a given α and ε, $\epsilon(u)$ decreases with the larger x, that is, the smaller x is, the more serious the problem is. Furthermore, for different functions, the fitting effect of functions with good properties is better than that of functions with poor properties.

7 Conclusion

In this paper, we study an inverse time-fractional Schrödinger problem of potential-free field. This problem is a serious ill-posed. Under a priori assumption, we obtain the optimal error bound result. A modified kernel method is introduced to prove the convergence estimate obtained under the priori regularization parameter selection rule is optimal, and the convergence estimate obtained under the posteriori regularization parameter selection rule is order-optimal. Three numerical examples are given to illustrate the effectiveness, stability and superiority of this method.

Disclosure statement

No potential conflict of interest was reported by the author.

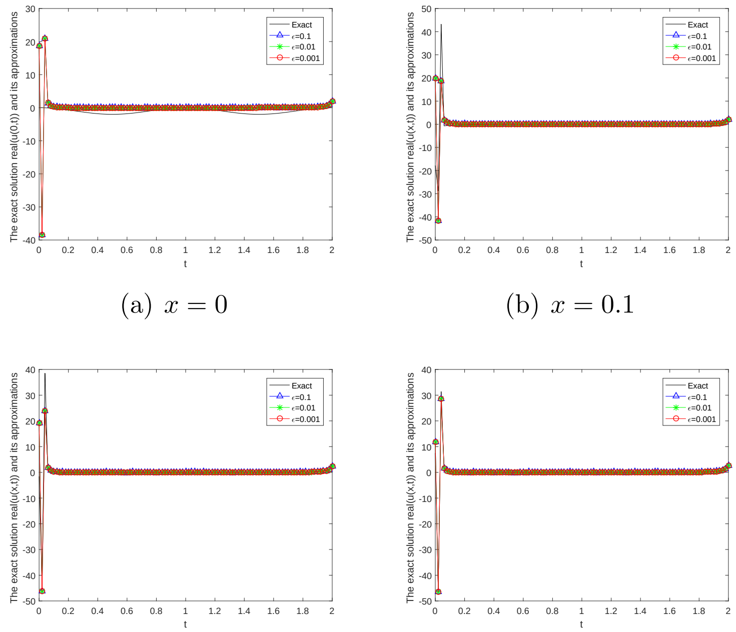

(a) $x = 0$ (b) $x = 0.1$

(c) $x = 0.5$ (d) $x = 0.9$

Figure 1: The real part of the exact solution and its approximation solution for Example 1 with $\alpha = 0.1$ and $\varepsilon = 0.1, 0.01, 0.001$.

References

[1] M. S. D. Bianchi, M. D. Ventra, Differential equations and factorization property for the one-dimensional schrodinger equation with position-dependent mass, European. J. Phys. 16 (6) (1995) 260–265.

[2] D. A. Dianawati, A. Suparmi, C. Cari, Y. Mohtar, Relativistic energy analysis for d-dimensional dirac equation with eckart plus hulthen central potential coupled by modified yukawa tensor potential using romanovski polynomial method, J. Phys. Conf. Ser. 776 (1) (2016) 012093.

[3] A. G. Bratsos, A linearized finite-difference scheme for the numerical solution of the nonlinear cubic schrӧdinger equation, J. Comput. Appl. Math. 8 (3) (2001) 459–467.

[4] A. Bratsos, M. Ehrhardt, I. T. Famelis, A discrete adomian decomposition method for discrete nonlinear schrӧdinger equations, Appl. Math. Comput. 197 (1) (2008) 190–205.

[5] N. H. Sweilam, Variational iteration method for solving cubic nonlinear schrӧdinger equation, J. Comput. Appl. Math. 207 (1) (2007) 155–163.

[6] A. Korkmaz, I. Dağ, A differential quadrature algorithm for nonlinear schrӧdinger equation, Nonlinear Dyn. 56 (1-2) (2009) 69–83.

[7] T. S. El-Danaf, M. A. Ramadan, E. I. A. Alaal, Numerical studies of the cubic non-linear schrӧdinger equation, Nonlinear Dyn. 67 (1) (2012) 619–627.

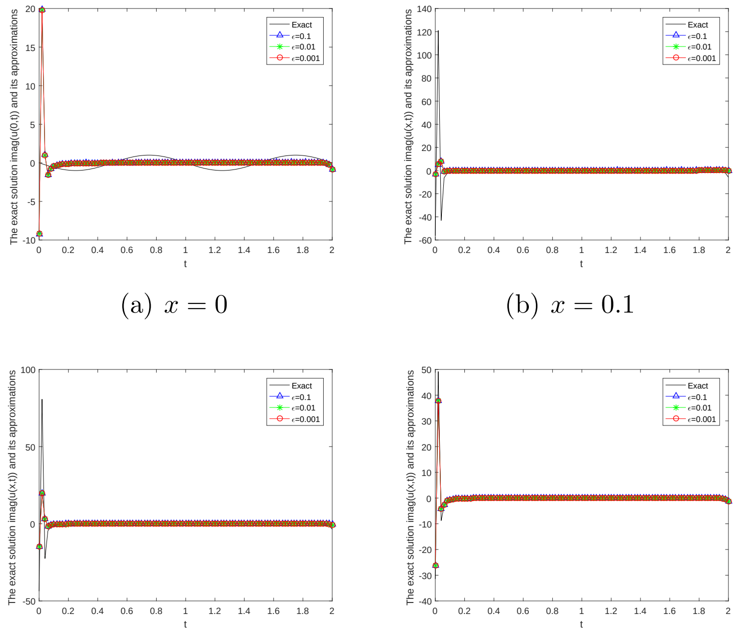

(a) $x = 0$ (b) $x = 0.1$

(c) $x = 0.5$ (d) $x = 0.9$

Figure 2: The imaginary part of the exact solution and its approximation solution for Example 1 with $\alpha = 0.1$ and $\varepsilon = 0.1, 0.01, 0.001$.

[8] B. Lin, Parametric cubic spline method for the solution of the nonlinear schr$\ddot{o}$dinger equation, Comput. Phys. Commun. 184 (1) (2013) 60–65.

[9] A. Taleei, M. Dehghan, Time-splitting pseudo-spectral domain decomposition method for the soliton solutions of the one- and multi-dimensional nonlinear schr$\ddot{o}$dinger equations, Comput. Phys. Commun. 185 (6) (2014) 1515–1528.

[10] T. Das, Bound state solutions of square root power law potential-wavefunction ansatz method on d-dimensional schr$\ddot{o}$dinger equation, Electron. J. Theor. Phys. 13 (36) (2016) 199–206.

[11] S. H. Dong, On the solutions of the schr$\ddot{o}$dinger equation with some anharmonic potentials: Wave function ansatz, Phys. Scr. 65 (4) (2002) 289–295.

[12] F. Yasuk, C. Berkdemir, A. Berkdemir, Exact solutions of the schr$\ddot{o}$dinger equation with non central potential by nikiforov uvarov method, J. Phys. A. Gen. Phys. 38 (29) (2005) 6579–6586.

[13] D. Mikulski, J. Konarski, K. Eder, M. Molski, S. Kabaci$\acute{n}$ski, Exact solution of the schr$\ddot{o}$dinger equation with a new expansion of anharmonic potential with the use of the supersymmetric quantum mechanics and factorization method, J. Math. Chem. 53 (9) (2015) 2018–2027.

[14] R. Kumar, F. Chand, Asymptotic study to the n-dimensional radial schr$\ddot{o}$dinger equation for the quark-antiquark system, Commun. Throe. Phys. 59 (5) (2013) 528–532.

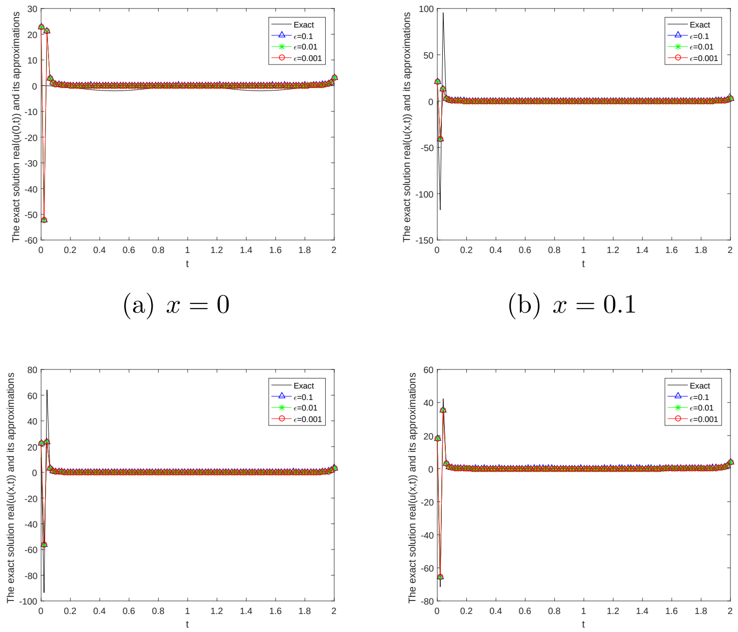

(a) $x = 0$ (b) $x = 0.1$

(c) $x = 0.5$ (d) $x = 0.9$

Figure 3: The real part of the exact solution and its approximation solution for Example 1 with $\alpha = 0.5$ and $\varepsilon = 0.1, 0.01, 0.001$.

[15] T. Das, Analytical approximate bound state solution of schr$\ddot{o}$dinger equation in d-dimensions with a new mixed class of potential for arbitrary-state via asymptotic iteration method, Chinese J. Phys. 54 (5) (2016) 850–858.

[16] G. Eskin, Inverse problems for the schr$\ddot{o}$dinger equations with time-dependent electromagnetic potentials and the aharonov-bohm effect, J. Math. Phys. 49 (2) (2008) 022105.

[17] W. S. Rakesh, Uniqueness for an inverse problems for the wave equation, Commun. Part. Diff. Eq. 13 (1) (1988) 87–96.

[18] R. Cipolatti, I. F. Lopez, Determination of coefficients for a dissipative wave equation via boundary measurements, J. Math. Anal. Appl. 306 (1) (2005) 317–329.

[19] J. Cheng, M. Yamamoto, The global uniqueness for determining two convection coefficients from dirichlet to neumann map in two dimensions, Inverse Probl. 16 (3) (2000) L25–L30.

[20] R. M. Brown, R. M. Brown, G. A. Uhlmann, Uniqueness in the inverse conductivity problem for nonsmooth conductivities in two dimensions, Commun. Part. Diff. Eq. 22 (5-6) (1997) 1009–1027.

[21] A. L. Bukhgeim, Recovering a potential from cauchy data in the two-dimensional case, J. Invers Ill-Pose. Probl. 16 (1) (2008) 19–33.

[22] O. Y. Imanuvilov, M. Yamamoto, Inverse boundary value problem for schr$\ddot{o}$dinger equation in two dimensions, Siam J. Math. Anal. 44 (3) (2012) 1333–1339.

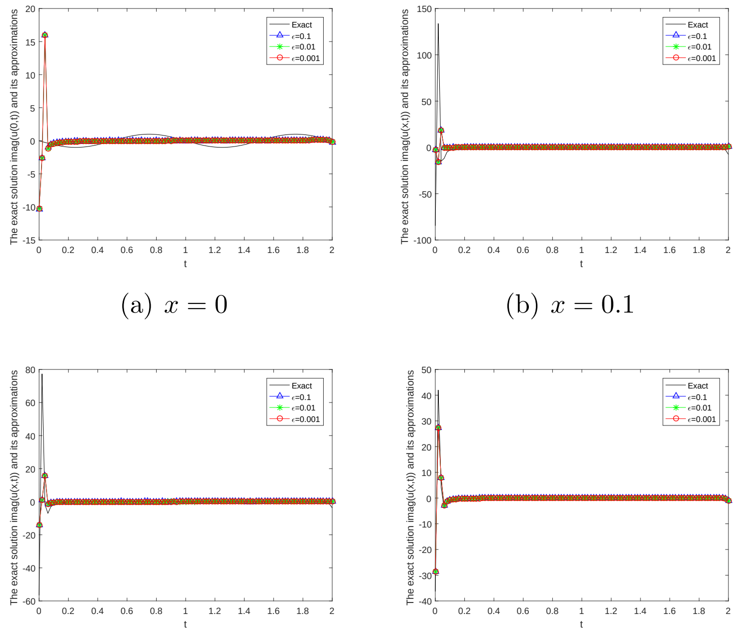

(a) $x = 0$ (b) $x = 0.1$

(c) $x = 0.5$ (d) $x = 0.9$

Figure 4: The imaginary part of the exact solution and its approximation solution for Example 1 with $\alpha = 0.5$ and $\varepsilon = 0.1, 0.01, 0.001$.

[23] A. I. Nachman, Global uniqueness for a two-dimensional inverse boundary value problem, Ann. Math. 143 (1) (1996) 71–96.

[24] M. Santacesaria, Global stability for the multi-channel gel'fandccalder$\acute{o}$n inverse problem in two dimensions, B. Sci. Math. 136 (7) (2012) 731–744.

[25] N. Laskin, Fractional quantum mechanics and l$\acute{e}$vy path integrals, Phys. Lett. A 268 (4) (1999) 298–305.

[26] M. Naber, Time fractional schrodinger equation, J. Math. Phys. 45 (8) (2004) 3339–3352.

[27] A. Ashyralyev, B. Hicdurmaz, On the numerical solution of fractional parabolic partial differential equations with the dirichlet condition, Int. J. Comput. Math. 89 (13-14) (2012) 1927–1936.

[28] R. Garrappa, I. Moret, M. Popolizio, Solving the time-fractional schr?dinger equation by krylov projection methods, J. Comput. Phys. 293 (2015) 115–134.

[29] J. G. Wang, T. Wei, Y. B. Zhou, Tikhonov regularization method for a backward problem for the time-fractional diffusion equation, Appl. Math. Model. 37 (18-19) (2013) 8518–8532.

[30] X. Feng, L. Eld$\acute{e}$n, Solving a cauchy problem for a 3d elliptic pde with variable coefficients by a quasi-boundary-value method, Inverse Probl. 30 (1) (2014) 015005.

[31] H. W. Zhang, H. H. Qin, T. Wei, A quasi-reversibility regularization method for the cauchy problem of the helmholtz equation., Int. J. Comput. Math. 88 (4) (2011) 839–850.

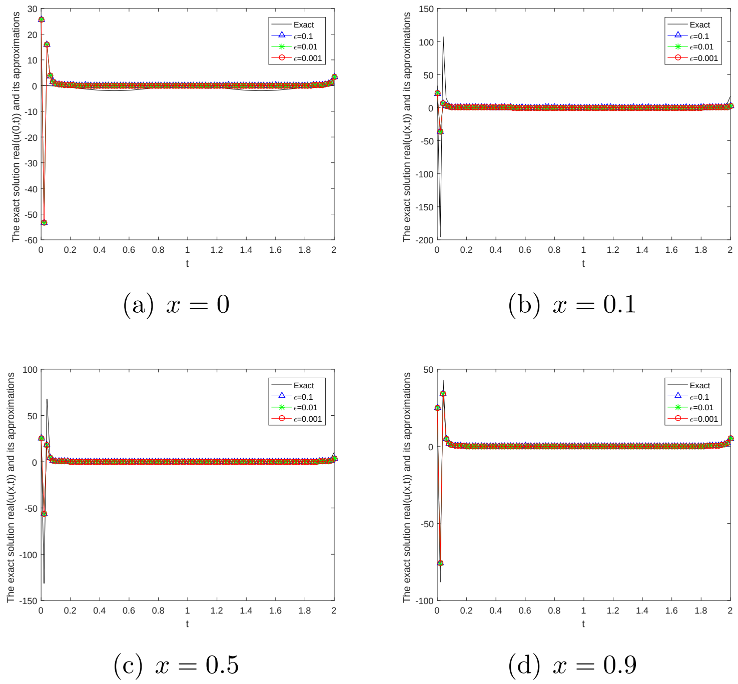

(a) $x = 0$ (b) $x = 0.1$

(c) $x = 0.5$ (d) $x = 0.9$

Figure 5: The real part of the exact solution and its approximation solution for Example 1 with $\alpha = 0.8$ and $\varepsilon = 0.1, 0.01, 0.001$.

[32] F. Yang, C. L. Fu, The quasi-reversibility regularization method for identifying the unknown source for time fractional diffusion equation, Appl. Math. Model. 39 (5-6) (2015) 1500–1512.

[33] F. Yang, C. L. Fu, X. X. Li, A mollification regularization method for unknown source in time-fractional diffusion equation, Int. J. Comput. Math. 91 (7) (2014) 1516–1534.

[34] X. T. Xiong, C. L. Fu, H. F. Li, Fourier regularization method of a sideways heat equation for determining surface heat flux, J. Math. Anal. Appl. 317 (1) (2006) 331–348.

[35] X. X. Li, J. L. Lei, F. Yang, An a posteriori fourier regularization method for identifying the unknown source of the space-fractional diffusion equation, J. Inequal. Appl. 2014 (1) (2014) 1–13.

[36] Y. Fan, C. L. Fu, X. X. Li, The fourier regularization method for identifying the unknown source for the modified helmholtz equation, Acta. Math. Sci. 34 (4) (2014) 1040–1047.

[37] F. Yang, Y. P. Ren, X. X. Li, Landweber iteration regularization method for identifying unknown source on a columnar symmetric domain, Inverse Probl. Sci. Eng. 26 (8) (2017) 1–21.

[38] F. Yang, X. Liu, X. X. Li, Landweber iterative regularization method for identifying the unknown source of the modified helmholtz equation, Bound. Value Probl. 2017 (1) (2017) 1–16.

[39] Z. Q. Zhang, Y. J. Ma, A modified kernel method for numerical analytic continuation, Inverse Probl. Sci. Eng. 21 (5) (2013) 840–853.

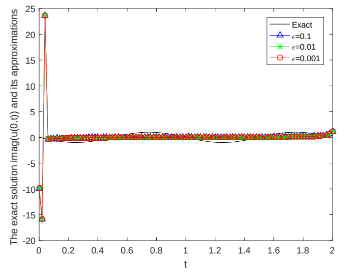

(a) $x = 0$

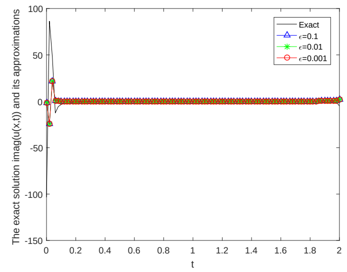

(b) $x = 0.1$

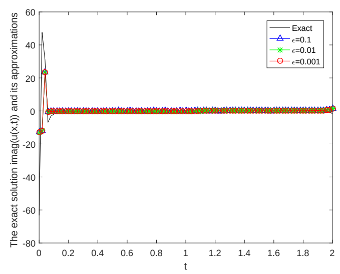

(c) $x = 0.5$

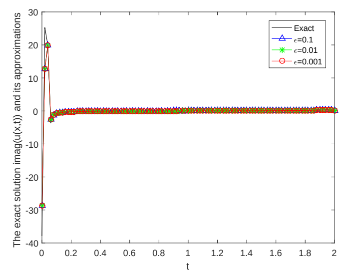

(d) $x = 0.9$

Figure 6: The imaginary part of the exact solution and its approximation solution for Example 1 with $\alpha = 0.8$ and $\varepsilon = 0.1, 0.01, 0.001$.

[40] M. I. Ivanchov, The inverse problem of determining the heat source power for a parabolic equation under arbitrary boundary conditions, J. Math. Sci. 88 (3) (1998) 432–436.

[41] T. Schröer, U. Tautenhahn, On the 'optimal' regularization methods for solving linear ill-posed problems, Z. Anal. Anwend 13 (4) (1994) 697–710.

[42] U. Tautenhahn, Optimal stable approximations for the sideways heat equation, J. Invers Ill-Pose. Probl. 5 (3) (1997) 287–307.

[43] U. Tautenhahn, Optimality for ill-posed problems under general source conditions, Numer. Funct. Anal. Optim. 19 (3-4) (1998) 377–398.

[44] G. Vainikko, On the optimality of methods for ill-posed problems, Z. Anal. Anwend. 6 (4) (1987) 351–362.

[45] H. W. Engl, M. Hanke, A. Neubauer, Regularization of Inverse Problem, MA, Kluwer Academic, Boston, 1996.

[46] U. Tautenhahn, R. Gorenflo, On optimal regularization methods for fractional differentiation, J. Anal. Appl. 18 (2) (1999) 449–467.

[47] F. F. Dou, C. L. Fu, F. L. Yang, Optimal error bound and fourier regularization for identifying an unknown source in the heat equation, J. Comput. Appl. Math. 230 (2) (2009) 728–737.

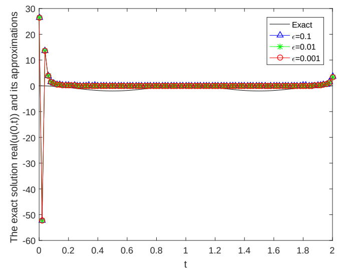

(a) $x = 0$

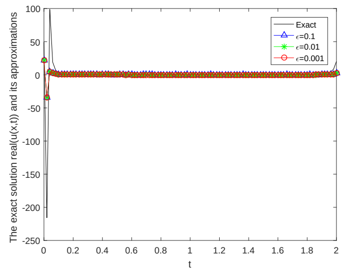

(b) $x = 0.1$

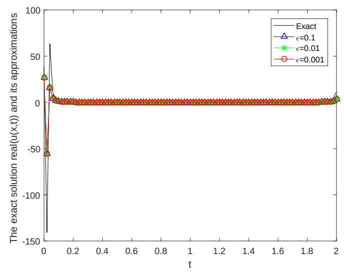

(c) $x = 0.5$

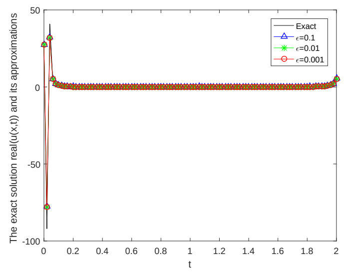

(d) $x = 0.9$

Figure 7: The real part of the exact solution and its approximation solution for Example 1 with $\alpha = 0.9$ and $\varepsilon = 0.1, 0.01, 0.001$.

[48] A. Kirseh, An lntroduction to the mathematic theory of inverse problem, Springer, New York, 1996.

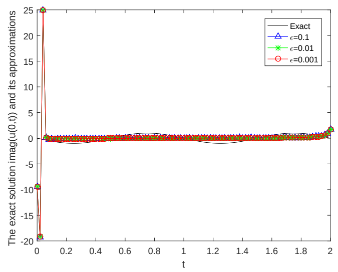

(a) $x = 0$

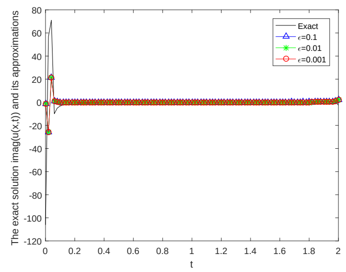

(b) $x = 0.1$

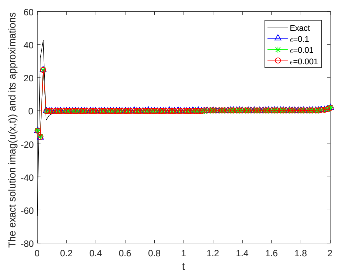

(c) $x = 0.5$

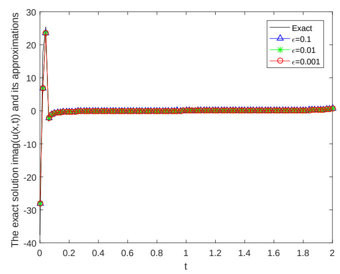

(d) $x = 0.9$

Figure 8: The imaginary part of the exact solution and its approximation solution for Example 1 with $\alpha = 0.9$ and $\varepsilon = 0.1, 0.01, 0.001$.

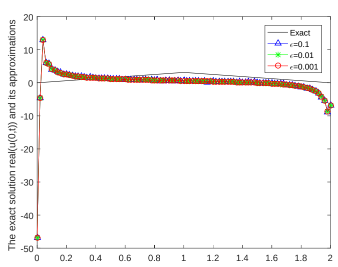

(a) $x = 0$

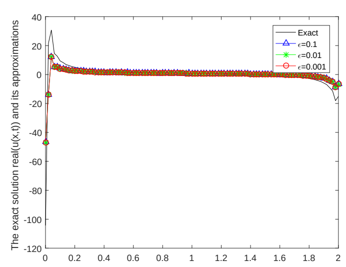

(b) $x = 0.1$

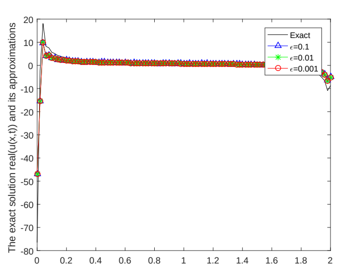

(c) $x = 0.5$

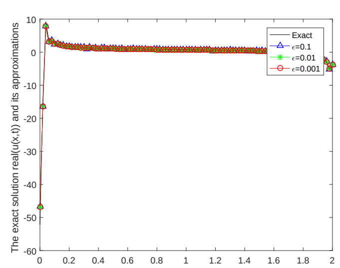

(d) $x = 0.9$

Figure 9: The real part of the exact solution and its approximation solution for Example 2 with $\alpha = 0.1$ and $\varepsilon = 0.1, 0.01, 0.001$.

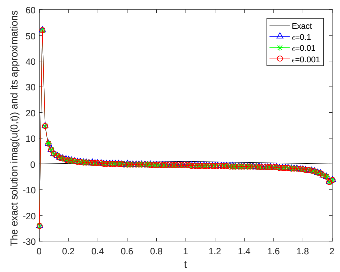

(a) $x = 0$

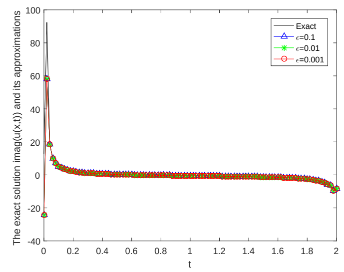

(b) $x = 0.1$

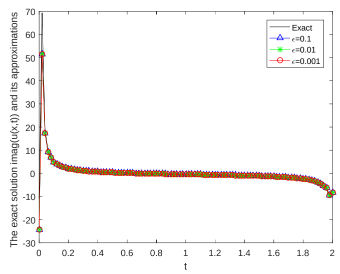

(c) $x = 0.5$

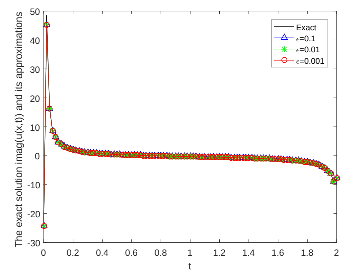

(d) $x = 0.9$

Figure 10: The imaginary part of the exact solution and its approximation solution for Example 2 with $\alpha = 0.1$ and $\varepsilon = 0.1, 0.01, 0.001$.

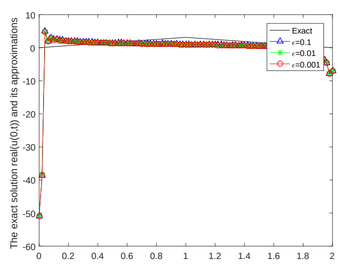

(a) $x = 0$

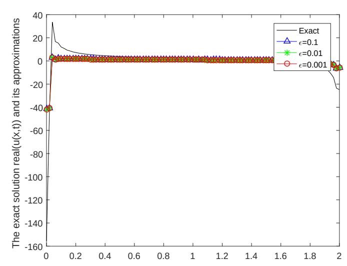

(b) $x = 0.1$

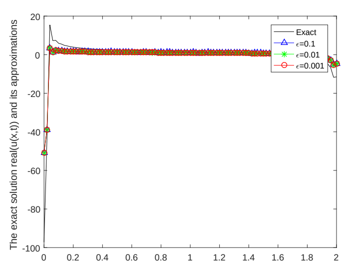

(c) $x = 0.5$

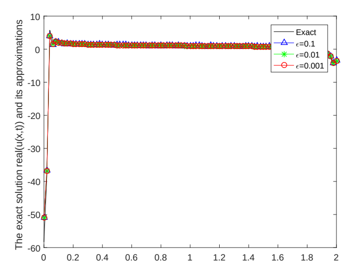

(d) $x = 0.9$

Figure 11: The real part of the exact solution and its approximation solution for Example 2 with $\alpha = 0.5$ and $\varepsilon = 0.1, 0.01, 0.001$.

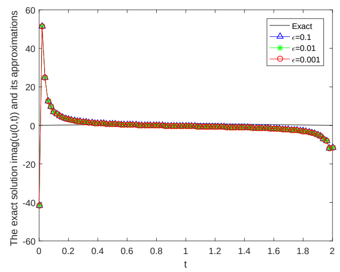

(a) $x = 0$

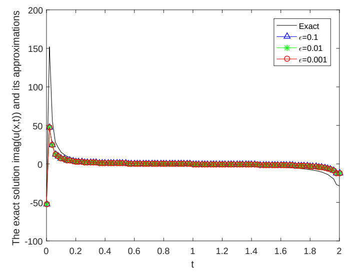

(b) $x = 0.1$

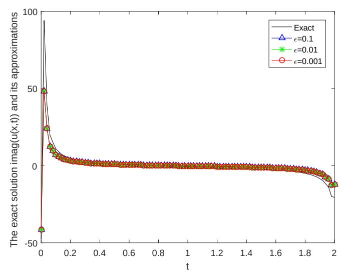

(c) $x = 0.5$

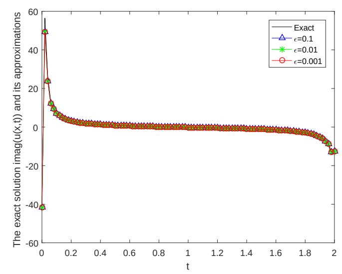

(d) $x = 0.9$

Figure 12: The imaginary part of the exact solution and its approximation solution for Example 2 with $\alpha = 0.5$ and $\varepsilon = 0.1, 0.01, 0.001$.

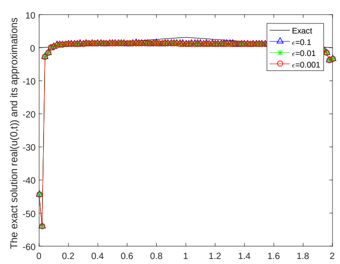

(a) $x = 0$

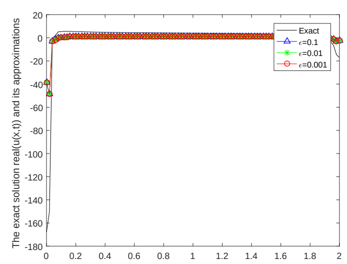

(b) $x = 0.1$

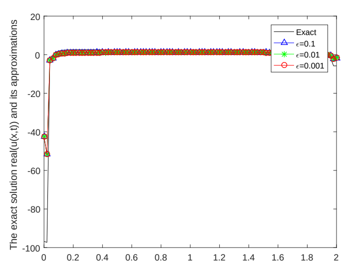

(c) $x = 0.5$

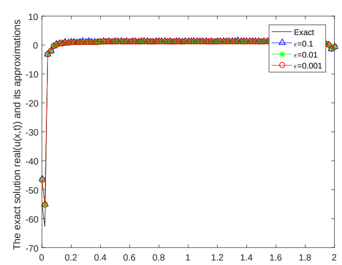

(d) $x = 0.9$

Figure 13: The real part of the exact solution and its approximation solution for Example 2 with $\alpha = 0.8$ and $\varepsilon = 0.1, 0.01, 0.001$.

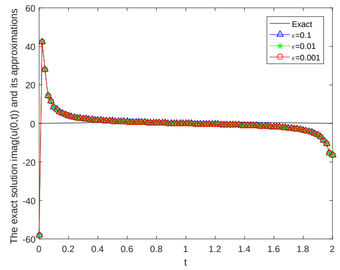

(a) $x = 0$

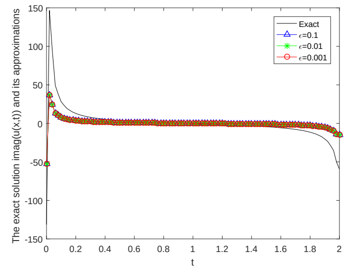

(b) $x = 0.1$

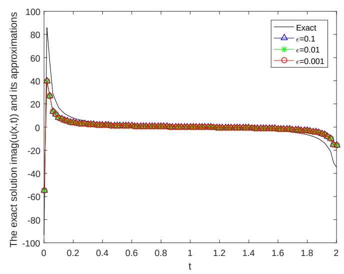

(c) $x = 0.5$

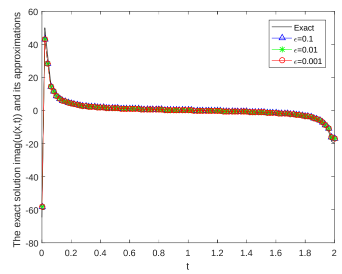

(d) $x = 0.9$

Figure 14: The imaginary part of the exact solution and its approximation solution for Example 2 with $\alpha = 0.8$ and $\varepsilon = 0.1, 0.01, 0.001$.

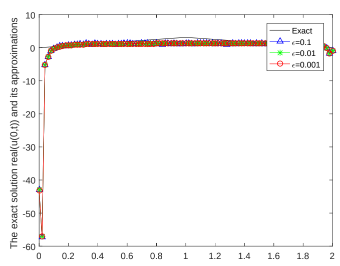

(a) $x = 0$

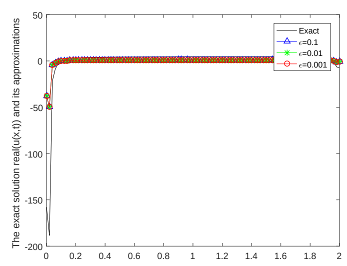

(b) $x = 0.1$

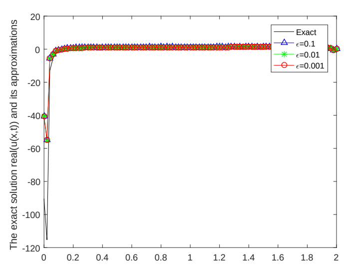

(c) $x = 0.5$

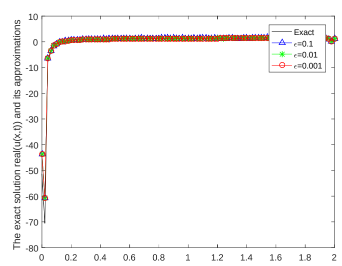

(d) $x = 0.9$

Figure 15: The real part of the exact solution and its approximation solution for Example 2 with $\alpha = 0.9$ and $\varepsilon = 0.1, 0.01, 0.001$.

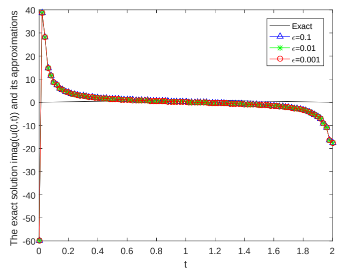

(a) $x = 0$

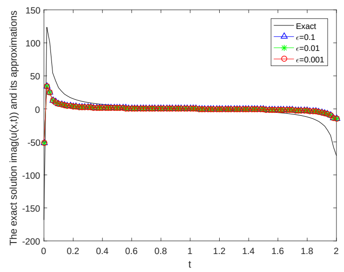

(b) $x = 0.1$

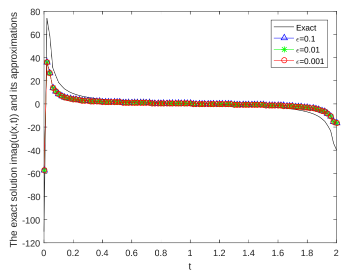

(c) $x = 0.5$

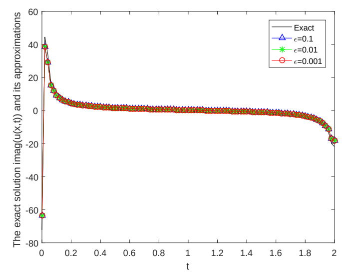

(d) $x = 0.9$

Figure 16: The imaginary part of the exact solution and its approximation solution for Example 2 with $\alpha = 0.9$ and $\varepsilon = 0.1, 0.01, 0.001$.

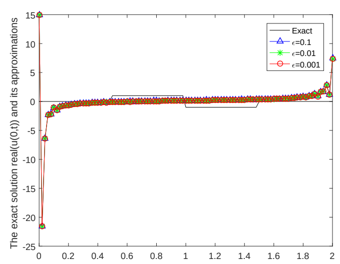

(a) $x = 0$

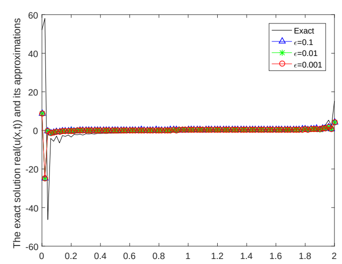

(b) $x = 0.1$

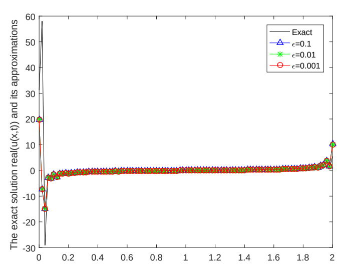

(c) $x = 0.5$

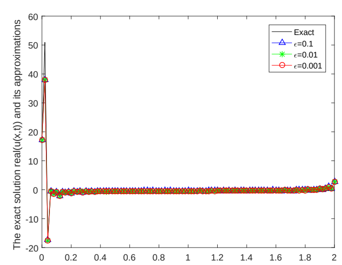

(d) $x = 0.9$

Figure 17: The real part of the exact solution and its approximation solution for Example 3 with $\alpha = 0.1$ and $\varepsilon = 0.1, 0.01, 0.001$.

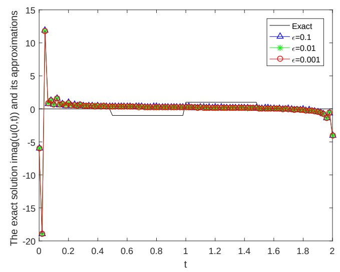

(a) $x = 0$

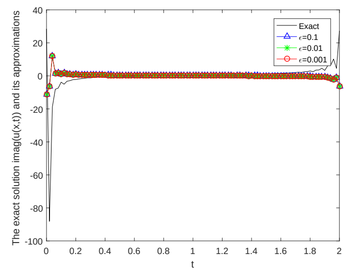

(b) $x = 0.1$

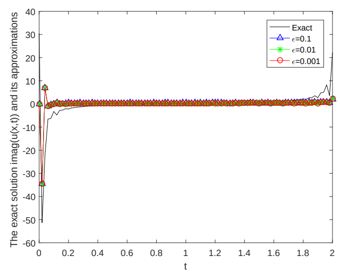

(c) $x = 0.5$

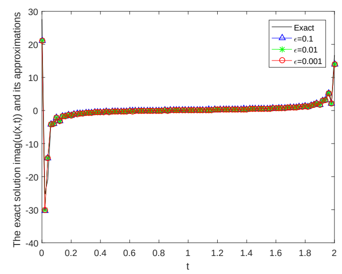

(d) $x = 0.9$

Figure 18: The imaginary part of the exact solution and its approximation solution for Example 3 with $\alpha = 0.1$ and $\varepsilon = 0.1, 0.01, 0.001$.

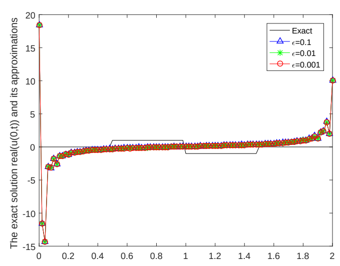

(a) $x = 0$

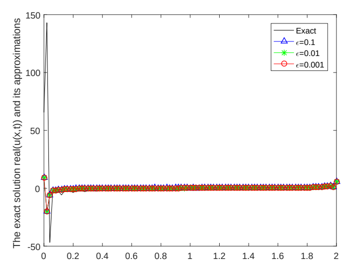

(b) $x = 0.1$

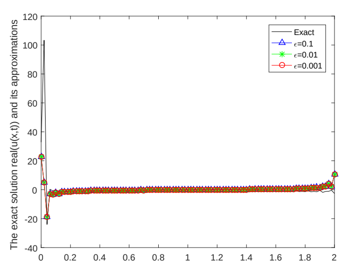

(c) $x = 0.5$

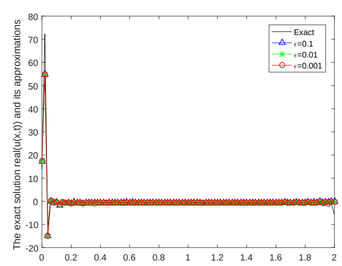

(d) $x = 0.9$

Figure 19: The real part of the exact solution and its approximation solution for Example 3 with $\alpha = 0.5$ and $\varepsilon = 0.1, 0.01, 0.001$.

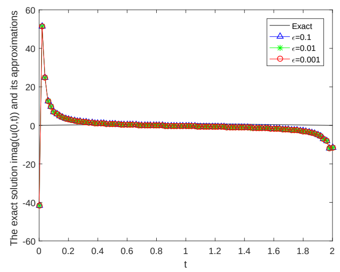

(a) $x = 0$

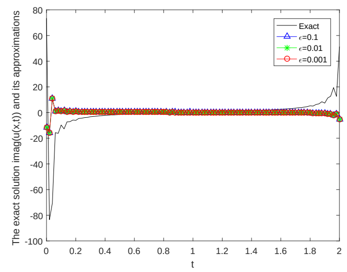

(b) $x = 0.1$

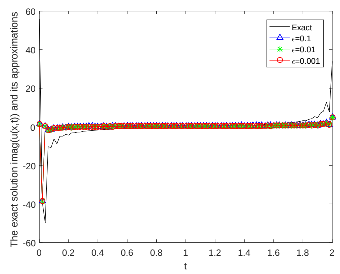

(c) $x = 0.5$

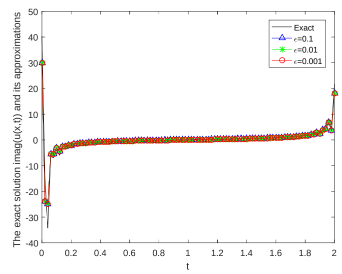

(d) $x = 0.9$

Figure 20: The imaginary part of the exact solution and its approximation solution for Example 3 with $\alpha = 0.5$ and $\varepsilon = 0.1, 0.01, 0.001$.

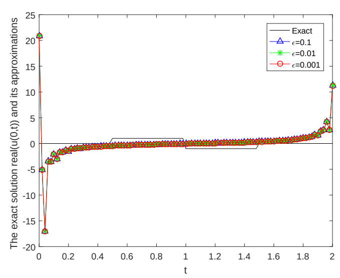

(a) $x = 0$

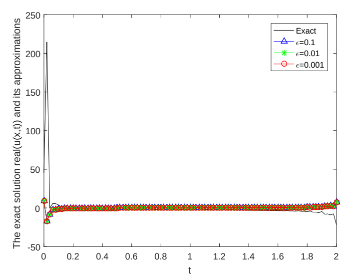

(b) $x = 0.1$

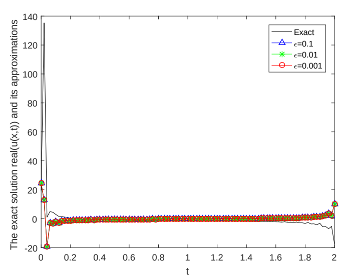

(c) $x = 0.5$

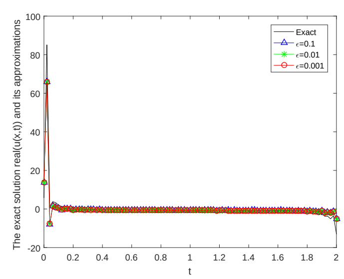

(d) $x = 0.9$

Figure 21: The real part of the exact solution and its approximation solution for Example 3 with $\alpha = 0.8$ and $\varepsilon = 0.1, 0.01, 0.001$.

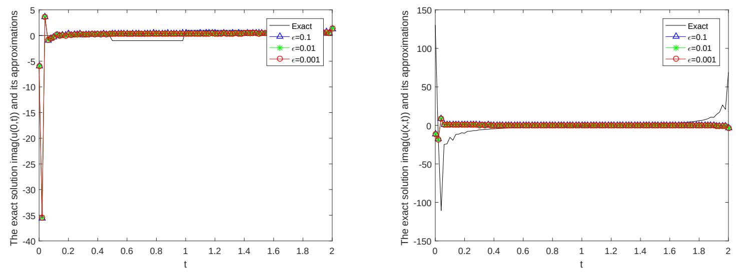

(a) $x = 0$ (b) $x = 0.1$

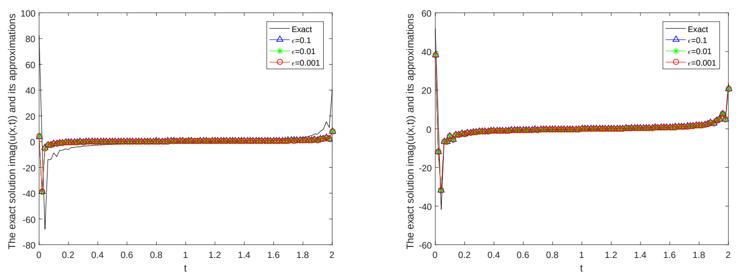

(c) $x = 0.5$ (d) $x = 0.9$

Figure 22: The imaginary part of the exact solution and its approximation solution for Example 3 with $\alpha = 0.8$ and $\varepsilon = 0.1, 0.01, 0.001$.

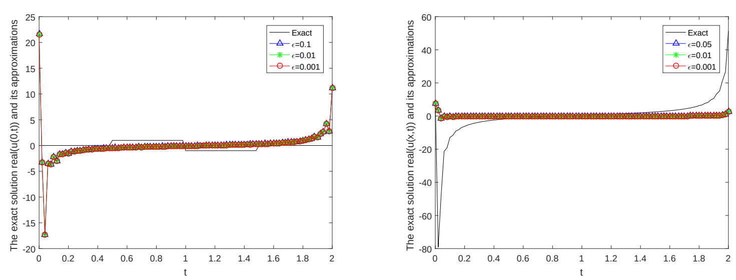

(a) $x = 0$ (b) $x = 0.1$

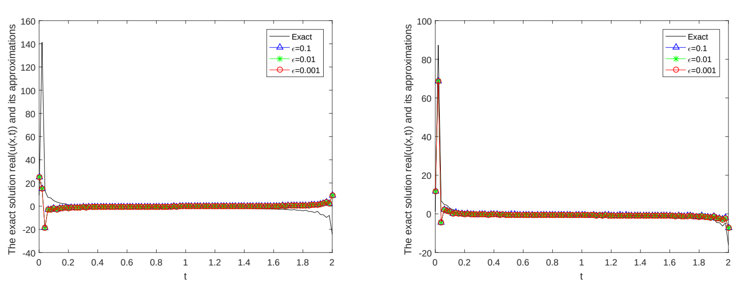

(c) $x = 0.5$ (d) $x = 0.9$

Figure 23: The real part of the exact solution and its approximation solution for Example 3 with $\alpha = 0.9$ and $\varepsilon = 0.1, 0.01, 0.001$.

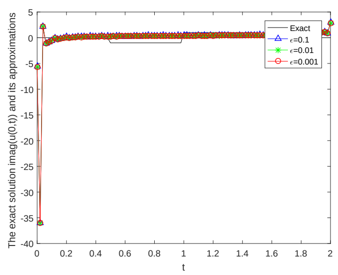

(a) $x = 0$

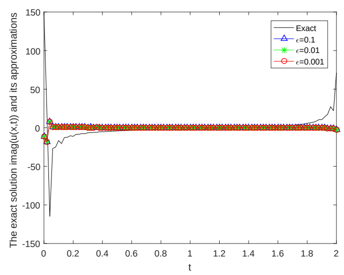

(b) $x = 0.1$

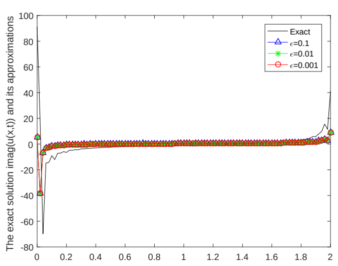

(c) $x = 0.5$

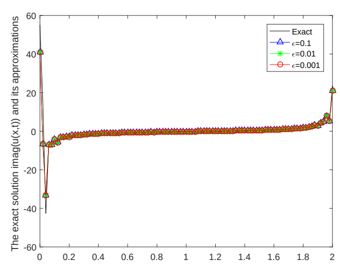

(d) $x = 0.9$

Figure 24: The imaginary part of the exact solution and its approximation solution for Example 3 with $\alpha = 0.9$ and $\varepsilon = 0.1, 0.01, 0.001$.